UNIVERSIDADE ESTADUAL DE CAMPINAS
FACULDADE DE ODONTOLOGIA DE PIRACICABA

HELOISA NAVARRO PANTAROTO

REVESTIMENTO DE TiO_2 CRISTALINO NA SUPERFÍCIE DO TITÂNIO: ESTABILIDADE ELETROQUÍMICA E PROPRIEDADES BIOLÓGICAS

CRYSTALLINE TiO_2 COATING ON TITANIUM SURFACE: ELETROCHEMICAL STABILITY AND BIOLOGICAL PROPERTIES

Piracicaba

2020

HELOISA NAVARRO PANTAROTO

REVESTIMENTO DE TiO_2 CRISTALINO NA SUPERFÍCIE DO TITÂNIO: ESTABILIDADE ELETROQUÍMICA E PROPRIEDADES BIOLÓGICAS

CRYSTALLINE TiO_2 COATING ON TITANIUM SURFACE: ELETROCHEMICAL STABILITY AND BIOLOGICAL PROPERTIES

Tese apresentada à Faculdade de Odontologia de Piracicaba da Universidade Estadual de Campinas como parte dos requisitos exigidos para a obtenção do título de Doutora em Clínica Odontológica, na Área de Prótese dental.

Thesis presented to the Piracicaba Dental School of the University of Campinas in partial fulfillment of the requirements for the degree of Doctor in Dental Clinic, in Dental Prosthesis area.

Orientador: Prof. Dr. Valentim Adelino Ricardo Barão

Este exemplar corresponde à versão final da tese defendida pela aluna Heloisa Navarro Pantaroto e orientada pelo Prof. Dr. Valentim Adelino Ricardo Barão.

Piracicaba
2020

Ficha catalográfica
Universidade Estadual de Campinas
Biblioteca da Faculdade de Odontologia de Piracicaba
Marilene Girello - CRB 8/6159

P195r

Pantaroto, Heloisa Navarro, 1991-
Revestimento de TiO_2 cristalino na superfície do titânio : estabilidade eletroquímica e propriedades biológicas / Heloisa Navarro Pantaroto. – Piracicaba, SP : [s.n.], 2020.

Orientador: Valentim Adelino Ricardo Barão.
Tese (doutorado) – Universidade Estadual de Campinas, Faculdade de Odontologia de Piracicaba.

1. Titânio. 2. Implantes dentários. 3. Corrosão. 4. Terapia ultravioleta. 5. Osteoblastos. I. Barão, Valentim Adelino Ricardo, 1983-. II. Universidade Estadual de Campinas. Faculdade de Odontologia de Piracicaba. III. Título.

Informações para Biblioteca Digital

Título em outro idioma: Crystalline TiO_2 coating on titanium surface : eletrochemical stability and biological properties
Palavras-chave em inglês:
Titanium
Dental implants
Corrosion
Ultraviolet therapy
Osteoblasts
Área de concentração: Prótese Dental
Titulação: Doutora em Clínica Odontológica
Banca examinadora:
Valentim Adelino Ricardo Barão [Orientador]
Érica Dorigatti De Avilla
Marcelo Ferraz Mesquita
Nilton Francelosi Azevedo Neto
Karina Gonzales Silverio Ruiz
Data de defesa: 27-02-2020
Programa de Pós-Graduação: Clínica Odontológica

Identificação e informações acadêmicas do(a) aluno(a)
- ORCID do autor: https://orcid.org/0000-0001-7391-2025
- Currículo Lattes do autor: http://lattes.cnpq.br/2772569859102227

UNIVERSIDADE ESTADUAL DE CAMPINAS
Faculdade de Odontologia de Piracicaba

A Comissão Julgadora dos trabalhos de Defesa de Tese de Doutorado, em sessão pública realizada em 27 de fevereiro de 2020, considerou a candidata HELOISA NAVARRO PANTAROTO aprovada.

PROF. DR. VALENTIM ADELINO RICARDO BARÃO

PROF. DR. NILTON FRANCELOSI AZEVEDO NETO

PROFª. DRª. ÉRICA DORIGATTI DE AVILA

PROF. DR. MARCELO FERRAZ MESQUITA

PROFª. DRª. KARINA GONZALES SILVERIO RUIZ

A Ata da defesa, assinada pelos membros da Comissão Examinadora, consta no SIGA/Sistema de Fluxo de Dissertação/Tese e na Secretaria do Programa da Unidade.

DEDICATÓRIA

Aos meus pais Pedro e Rosemeire e aos meus irmãos João e Luciana

O apoio de vocês é fundamental para mim. Obrigada por todo amor, educação, ensinamentos, companheirismo e paciência que sempre me dedicaram, eu sou eternamente grata por tudo isso. Vocês são os melhores exemplos que eu poderia ter e agradeço a Deus todos os dias por tê-los em minha vida. Amo muito vocês!

Aos meus avós José, Mathilde e ao meu Bisavô Gonçalo

Que sempre estiveram muito presentes durante toda minha vida, e agora estão presentes em meu coração. Vocês me deixaram muitas marcas e lembranças boas, e com certeza são a minha maior saudade!

AGRADECIMENTOS

Primeiramente eu agradeço a **Deus**, por sempre proteger e guiar as minhas escolhas. Por todo amparo, força e coragem durante momentos difíceis. Pela minha saúde e da minha família e por todo amor e carinho que recebo de todos meus familiares e amigos, que sem dúvida me incentivam a seguir em frente. Obrigada pela minha vida, por tudo que já conquistei e por todas as pessoas incríveis que estão à minha volta

Ao meu orientador **Profº Dr. Valentim Adelino Ricardo Barão**. Muito obrigada pela oportunidade de ser sua orientada, pelos ensinamentos transmitidos e por sua disponibilidade. Sua paixão pela pesquisa é evidente e incentivadora, bem como a atenção com que trata seus alunos. Sem dúvida, um grande exemplo a ser seguido. Sinto-me privilegiada em ser sua orientada.

A **Universidade Estadual de Campinas – UNICAMP**, na pessoa do Magnífico Reitor, **Prof. Dr. Marcelo Knobel**, pelo meu doutorado nesta instituição.

A **Faculdade de Odontologia de Piracicaba – UNICAMP**, na pessoa do seu Diretor **Prof. Dr. Francisco Haiter Neto.**

A Coordenadora Geral da Pós-Graduação **Profa. Dra. Karina Gonzales Silvério Ruiz** e a Coordenadora do Programa de Pós-Graduação em Clínica Odontológica **Prof. Dr. Valentim Adelino Ricardo Barão.**

A **Coordenação de Aperfeiçoamento de Pessoal de Nível Superior – Brasil (CAPES)** - Código de Financiamento 001, pela concessão do auxílio de financiamento do projeto.

Ao **Laboratório de Plasmas Tecnológicos da Universidade Estadual Paulista "Júlio de Mesquita Filho" – UNESP (Campus de Sorocaba)**, representado pelo **Prof. Dr. Nilson Cristino da Cruz** e pela **Prof. Dra. Elidiane Cipriano Rangel** pela parceria no desenvolvimento deste trabalho.

Ao **Laboratório de Física da Universidade Estadual Paulista "Júlio de Mesquita Filho" – UNESP (Campus de Bauru)**, representado pelo **Prof. Dr. José Humberto Dias da Silva** pela parceria no desenvolvimento deste trabalho.

Ao **Laboratório de Física da Universidade Estadual de Campinas – UNICAMP,** representado pelo **Prof. Dr. Richard Landers** pela parceria no desenvolvimento deste trabalho.

Ao **Laboratório de Bioquímica Oral da FOP – UNICAMP**, representado pelo **Prof. Dr. Jaime Aparecido Cury** pela parceria no desenvolvimento deste trabalho.

Ao **Laboratório de Periodontia da FOP – UNICAMP**, representado pelo **Prof. Dr. Franscisco Humberto Nociti Júnior** pela parceria no desenvolvimento deste trabalho.

Ao **Centro Nacional de Pesquisa em Engenharia e Materiais (CNPEM)** e ao **Laboratório Nacional de Nanotecnologia (LNNano)**.

Ao **Centro de Microscopia e Imagem (CMI)** e ao técnico **Adriano Luis Martins**.

Ao **Prof. Dr. José Humberto Dias da Silva** (UNESP-Bauru) pela parceria no desenvolvimento deste estudo.

Ao **Prof. Dr. Renato Corrêa Viana Casarin** pela parceria no desenvolvimento deste estudo.

Aos docentes **Prof. Dr. Marcelo Ferraz Mesquita, Prof. Dr. Rafael Leonardo Xediek Consani, Prof. Dr. Mauro Nóbilo, Profa. Dra. Altair Del Bel Cury, Profa. Dra. Renata Cunha Matheus Rodrigues Garcia, Prof. Dr. Wander José da Silva** por todo conhecimento compartilhado.

A Sra. **Eliete A. Ferreira Lima Marim**, secretária do Departamento de Prótese e Periodontia da FOP-UNICAMP, pela atenção e toda gentileza. Ao **Eduardo Pinez (Du),** técnico do Laboratório de Prótese Total, pelo bom humor, amizade e prontidão para ajudar.

Aos técnicos do **Laboratório de Bioquímica Oral, Waldomiro Vieira** e **José Alfredo da Silva,** por toda solicitude.

Ao **Nilton Francelosi** pelo treinamento nos equipamentos do Laboratório de Física (UNESP – Bauru), por todos os ensinamentos, conselhos, prestatividade e amizade.

Ao **Orisson Ponce Gomes** por sua contribuição e prestatividade neste trabalho.

A **Amanda Bandeira** por sua amizade e contribuição neste trabalho.

A minha família **Pedro**, **Rosemeire, João e Luciana** por tudo que sempre fizeram por mim e por todo amor com que me recebem. E em especial pela ajuda na confecção da caixa de luz que foi essencial neste trabalho.

A **Família Navarro e Família Pantaroto**, em especial às famílias da minha tia **Antonia**, tia **Leonilde,** à dos meus padrinhos **Robson, Izabel e Fabiana** e à família do meu tio **Mário**, por todo zelo, companheirismo e orações. O apoio e amor de vocês são e sempre serão essenciais para mim.

Ao **Rodrigo Panfiett**, por todo amor, apoio, compreensão e companheirismo.

A todos os meus amigos do Laboratório de Prótese Total **Adaias Oliveira Matos, Anna Gabriella Presotto, Bruna Nagay, Caroline Dini, Daniele Valente, Guilherme**

Borges, Halina Berejuk, Jairo Cordeiro, Letícia Del Rio, Marcos Pomini, Raphael Costa, Ricardo Caldas, Roberta Araújo, Thaís Barbin, Thamara Beline, Vitória Piccolli e todos os amigos da **Pós-Graduação** o meu muito obrigado pela boa convivência, amizade e experiências trocadas.

Aos amigos da pós-graduação **Bruna Guerra, Elis Lira, Hortência Xavier, Ingrid Andrade Meira, Jéssica Camassari, Lívia Nazareth, Louise Dornelas, Loyse Martorano, Mariana Souza, Mariana Itaborai, Maurício Guarda, Mayara Abreu, Olívia Figueiredo, Paolo Di Nizo, Raíra Brito, Raissa Machado, Renata Pereira, Rahyza Freire, Rodrigo Lins, Stephany Di Carla, Talita Carletti.**

Muito obrigada!

RESUMO

Os implantes dentários são comumente usados na reabilitação protética e o processo de osseointegração é mandatório para o sucesso e longevidade do tratamento. A osseointegracão envolve processos organizados, dos quais fazem parte proteínas, citocinas inflamatórias, células e a precipitação de hidroxiapatita. Todos esses processos podem ser influenciados pelas propriedades da superfície do implante. O titânio (Ti) e suas ligas são os materiais mais utilizados devido às suas adequadas propriedades mecânicas e biocompatibilidade. Tais propriedades são devidas à formação natural de uma camada instável de dióxido de titânio (TiO_2) na superfície, protetora ao processo de corrosão. Contudo, a bioatividade do Ti pode ser reduzida de acordo com o envelhecimento natural da superfície. Assim, foram propostos dois estudos *in vitro*: o desenvolvimento de um filme de TiO_2 estável e cristalino, a fim de melhorar as propriedades físico-químicas do Ti (1), seguido da fotofuncionalização por luz ultravioleta (UV), capaz de renovar a superfície (2). No primeiro estudo, filmes de TiO_2 pulverizados foram formados na superfície de Ti, com diferentes fases cristalinas (anatase, rutilo e fase mista). Os filmes foram avaliados quanto ao comportamento eletroquímico, propriedades de superfície, adsorção de proteína e precipitação da hidroxiapatita. Para isso, as superfícies foram caracterizadas quanto a composição química, topografia, fase cristalina e energia livre de superfície. Testes eletroquímicos foram conduzidos usando solução de fluido corpóreo (SFC). A adsorção de albumina foi medida pelo método do ácido bicinconínico. A precipitação da hidroxiapatita foi avaliada após 28 dias de imersão em SFC. Em geral, as fases cristalinas de TiO_2 apresentaram melhor comportamento eletroquímico, especialmente a mista, que apresentou a maior resistência à polarização ($p<0,05$). O rutilo apresentou maior diminuição da densidade de corrente e taxa de corrosão, enquanto a fase mista apresentou comportamento passivo mais estável ($p<0,05$). A fase mista aumentou a adsorção de albumina ($p<0,05$). A morfologia da hidroxiapatita foi dependente da fase cristalina, sendo mais evidente no grupo misto. A combinação das fases anatase e rutilo nos filmes de TiO_2 parece ser mais adequada para a aplicação em implantes, devido à maior proteção contra corrosão, maior adsorção de proteína e bioatividade. Assim, no segundo estudo, apenas a fase mista do TiO_2 foi usada para testar sua influência e da fotofuncionalização (meio de ativação da superfície) nas alterações físico-químicas de superfície e comportamento celular. As superfícies foram analisadas quanto à morfologia, topografia, composição química, fase cristalina e molhabilidade. Células pré-osteoblásticas (MC3T3E1) foram utilizadas para avaliar a morfologia, adesão, viabilidade, mineralização e expressão de citocinas (IFN-γ,

TNF-α, IL-4, IL-6 e IL-17). A fotofuncionalização aumentou a molhabilidade das superfícies tratadas com TiO_2 e não tratadas ($p<0,05$). O TiO_2 fotofuncionalizado apresentou maior adesão e viabilidade celular nos dias 2 e 4 ($p<0,05$). A fotofuncionalização potencializou essa viabilidade e induziu maior mineralização (dia 14) para ambas as superfícies ($p<0,05$). Em geral, as proteínas avaliadas foram levemente afetadas pelos tratamentos UV ou TiO_2. Assim, a incorporação de TiO_2 misto na superfície do Ti, seguida da fotofuncionalização por UV é promissora para aplicação em implantes dentários.

Palavras-chave: Titânio. Implantes dentários. Hidroxiapatitas. Corrosão. Proteínas sanguíneas. terapia ultravioleta. Osteoblastos. Citocinas.

ABSTRACT

Dental implants are commonly used in prosthetic rehabilitation, and the osseointegration is mandatory for the success and longevity of the treatment. The osseointegration process involves organized mechanisms, in which proteins, inflammatory cytokines, cells and hydroxyapatite orchestrate such process. These mechanisms can be governed by the surface properties of an implant material. Titanium (Ti) and its alloys are the most used material due to their adequate mechanical properties and bioactivity. Such properties are due to the unstable titanium dioxide oxide (TiO_2) naturally formed on its surface, which is protective to the corrosion process. Furthermore, the bioactivity of Ti can be reduced according to the natural aging of the surface. Thus, two *in vitro* studies were proposed: an incorporation of a stable and crystalline TiO_2 film to improve the physical-chemical properties of Ti (1), followed by an ultraviolet light (UV) photofunctionalization, which is able to renew the surface (2). In the first study, sputtered TiO_2 films were grown on titanium (Ti) surface, with different crystalline phases (anatase, rutile and mixed phase). Films were evaluated regarding their electrochemical behavior, surface properties, protein adsorption and hydroxyapatite precipitation. The surfaces were characterized as chemical composition, topography, crystalline phase and surface free energy (SFE). Electrochemical tests were conducted using simulated body fluid (SBF). Albumin adsorption was measured by bicinchoninic acid method. Hydroxyapatite (HA) precipitation was evaluated after 28 days of immersion in SBF. In general, TiO_2 crystalline phases showed improved electrochemical behavior, specially mixed TiO_2 that showed the highest polarization resistance ($p<0.05$). Rutile phase exhibited a greater influence on decreasing the current density and corrosion rate, while the mixed phase displayed a more stable passive behavior ($p<0.05$). Regarding protein interaction, mixed phase increased the albumin adsorption ($p<0.05$). The morphology of HA was dependent to the crystalline phase, being more evident in the mixed group. The combination of anatase and rutile structures to generate TiO_2 films seems to be more suitable for biomedical implants application as greater corrosion protection, higher protein adsorption and bioactivity were accounted. Therefore, in the second study, we only used mixed TiO_2 phase to verify its influence and the photofunctionalization on the physical-chemical surface alterations and cell behavior. Surfaces were analyzed in terms of morphology, topography, chemical composition, crystalline phase and wettability. Pre-osteoblastic cells (MC3T3E1) were used to assess cell morphology and adhesion, viability, mineralization and cytokine expression (IFN-γ, TNF-α, IL-4, IL-6 and IL-17). Photofunctionalization increased the wettability of both surface

conditions ($p<0.05$). TiO_2-treated samples featured normal cell morphology and spreading, and greater cell viability at 2 and 4 days ($p<0.05$). UV potentiated such viability and induced higher mineralization (day 14) for both surfaces ($p<0.05$). In general, assessed proteins were found slightly affected by either UV or TiO_2 treatments. Thus, mixed TiO_2 incorporation on Ti surface followed by a UV photofunctionalization seems to be promising to be applied on dental implants.

Key words: Titanium. Dental implants. Corrosion. Blood proteins. Hydroxyapatites. Ultraviolet Therapy. Osteoblasts. Cytokines.

SUMÁRIO

1 INTRODUÇÃO

Os implantes apresentam um papel extremamente importante na reabilitação protética, e para o sucesso do tratamento, a osseointegração é mandatória. A cicatrização da ferida cirúrgica ocorre por meio de uma sequência de processos organizados (Terheyden *et al.* 2012). Este processo envolve a secreção de citocinas, que coordenam o processo de cicatrização juntamente com as proteínas e as células. A formação do novo tecido ósseo começa a partir da secreção da matriz de colágeno pelos osteoblastos (Terheyden *et al.* 2012), sendo crucial para a osseointegração (Cheng *et al.* 2015).

Entretanto, situações desfavoráveis para o tratamento com implantes dentários são comumente encontradas em pacientes, reduzindo as taxas de sucesso e longevidade do tratamento. Portanto, é de suma importância desenvolver métodos que possam acelerar o processo de cicatrização nas áreas que receberam implantes (Hatoko *et al.* 2019), e consequentemente, promover uma melhor adaptação dos tecidos duros e moles ao redor dos implantes e seus componentes, favorecendo assim, não só a função como também a estética.

O titânio (Ti) e suas ligas são os materiais mais comumente utilizados por apresentarem excelentes propriedades mecânicas e biocompatibilidade superior comparado às outras ligas (Kulkarni *et al.* 2015). Isto se deve à camada de óxido naturalmente formada sobre a sua superfície. Esta camada é extremamente fina (5–6 nm) (Bronze-Uhle *et al.* 2019) e é a responsável por proteger o Ti dos fluídos orais, reduzindo a liberação de íons (López *et al.* 2011).

Entretanto, mesmo apresentando esta camada de óxido protetora, o Ti não é capaz de evitar a corrosão a longo prazo (Bronze-Uhle *et al.* 2019). O processo corrosivo nada mais é que a liberação de íons e os produtos de deterioração do material nos tecidos circundantes (Bayón *et al.* 2015; Fojt *et al.* 2013) podendo resultar em efeitos adversos no corpo (como osteólise, reabsorção óssea, infecções) e no implante (como a fratura) (Bayón *et al.* 2015; Bronze-Uhle *et al.* 2019). Quanto maior, mais compacta e mais estável for a camada de óxido, melhor será a resistência à corrosão do implante (Okazaki *et al.* 2005; Gabriel *et al.* 2012). Portanto, promover uma camada estável de dióxido de titânio (TiO_2) sobre a superfície do Ti pode ser interessante.

Outro fator a ser considerado é que o Ti é um material que está sujeito ao processo natural de envelhecimento da superfície, levando a uma perda em sua bioatividade (Att *et al.* 2009; Aita *et*

al. 2009). A fotofuncionalização é um método que vêm sendo proposto para revitalizar a superfície do Ti, resultando em um aumento da sua bioatividade (Att *et al.* 2009; Aita *et al.* 2009). Esta é um pré-tratamento na superfície do implante, no qual o implante é exposto à luz ultravioleta (UV) previamente à sua implantação, portanto, o paciente não é exposto à luz UV. As superfícies fotofuncionalizadas são conhecidas por serem osteocondutivas (Aita *et al.* 2009). Estudos *in vitro* e *in vivo* mostraram que a fotofuncionalização das superfícies do Ti maquinado ou com algum tratamento de superfície foi efetiva, promovendo a osseointegração da interface osso-implante de forma mais rápida e completa (Aita *et al.* 2009; Kawano *et al.* 2013; Hori *et al.* 2011; Zhang *et al.* 2017; Miyauchi *et al.* 2010; Leon-Ramos *et al.* 2019; Park *et al.* 2011; Hatoko *et al.* 2019; Shahramian *et al.* 2019). Isto ocorre, pois, este tratamento promove alterações na composição química e na molhabilidade da superfície (Att *et al.* 2009; Aita *et al.* 2009), o que aparentemente pode ser potencializado na presença do TiO_2 (Aita *et al.* 2009).

Sendo assim, o TiO_2 parece ser promissor tanto para aumentar a resistência à corrosão do Ti, como também para potencializar o efeito da fotofuncionalização desta superfície, revitalizando-a. O TiO_2 apresenta natureza polimórfica (Lim *et al.* 2014), exibindo duas principais fases cristalinas: a anatase e o rutilo, as quais aumentam a resistência do TiO_2 e também apresentam atividade fotocatalítica (Pantaroto *et al.* 2018), por isso podem potencializar o efeito da fotofuncionalização. Para incorporar o TiO_2 na superfície do Ti, diversos métodos podem ser realizados, como a técnica "*sol-gel*" (Ochsenbein *et al.* 2008; Shahramian *et al.* 2019), "*spin-coating*" (Westas *et al.* 2017), a anodização (Beltrán-Partida *et al.* 2017; Liu *et al.* 2017) e a pulverização catódica ou "*magnetron sputtering*" (Rupp 2012; Cao 2014; Pantaroto 2018). Esta última apresenta destaque, pois promove melhor adesão do filme à superfície, dureza e apresenta baixo custo (Choi *et al.* 2009; Yaghoubi *et al.* 2010; Cao *et al.* 2014; Lim *et al.* 2014). Além disso, na pulverização catódica há possibilidade de obtenção de filmes unicamente compostos de anatase ou rutilo, bem como formado pelas duas fases cristalinas (Mráz *et al.* 2011). Portanto, é um ótimo método para deposição do filme de TiO_2 nas suas diferentes fases cristalinas.

A incorporação do TiO_2 no Ti confere benefícios funcionais e estruturais (Lebre *et al.* 2017; Pantaroto *et al.* 2018), sendo um material promissor no campo biomédico devido à sua não toxicidade e propriedades não inflamatórias (Ahmed *et al.* 2011). Ademais, o pó de TiO_2 apresenta interação positiva com a proteína albumina, uma das mais abundantes proteínas presentes no plasma sanguíneo (Marucco *et al.* 2013). A adsorção de albumina é um fator chave

na biocompatibilidade dos implantes (Ahmed *et al.* 2011) e é considerada o primeiro acontecimento na superfície do biomaterial quando em contato com o sangue (Huang *et al.* 2003; Milleret *et al.* 2015; Roy *et al.* 2016; Shahramian *et al.* 2019). As proteínas inicialmente adsorvidas fazem uma cobertura sobre a superfície do implante, deixando-a apropriada para a adesão celular (Li *et al.* 2018) e consequentemente, integrando o implante aos tecidos circundantes.

Outro fator chave na implantodontia, é a habilidade do material para formação da hidroxiapatita (Gowtham *et al.* 2016) uma vez que isso mostra a habilidade do material se ligar ao osso (Kokubo *et al.* 2006), algo extremamente importante para a osseointegração. Além disso, o tamanho e formato da hidroxiapatita formada pode estimular as respostas inflamatórias após a sua implantação (Lebre *et al.* 2017). Portanto, é de suma importância investigarmos tanto a habilidade do material na formação de hidroxiapatita, quanto a morfologia da hidroxiapatita formada sobre a sua superfície (Lebre *et al.* 2017).

Assim, fica evidente que os filmes de TiO_2 podem apresentar um papel importante em vários fatores cruciais para o processo da osseointegração e consequentemente no sucesso e longevidade do tratamento reabilitador. Entretanto ainda não há um consenso na literatura sobre qual seria a melhor fase cristalina do TiO_2 para aplicação em implantes, considerando a técnica de pulverização catódica. Então, esta tese tem como objetivos:

(1) comparar as diferentes fases cristalinas nos filmes de TiO_2 obtidos pela técnica de pulverização catódica, considerando a resistência à corrosão, a adsorção de proteína, bem como a formação e morfologia da camada de hidroxiapatita;

(2) investigar a ação da fotofuncionalização na superfície do TiO_2 cristalino e delinear a influência do TiO_2 e da fotofuncionalização no comportamento de células pré-osteoblásticas (quanto à morfologia, adesão, viabilidade e mineralização) e na expressão de citocinas inflamatórias.

2 ARTIGOS

2.1 Artigo: Sputtered crystalline TiO_2 film drives improved surface properties of titanium-based biomedical implants

Heloisa Navarro Pantaroto[a], Jairo Matozinho Cordeiro[a,b], Lucas Toniolo Pereira[a], Elidiane Cipriano Rangel[c], Nilton Francelosi Azevedo Neto[d], Jose Humberto Dias da Silva[d], Valentim Adelino Ricardo Barão[a,b*]

[a] *University of Campinas (UNICAMP), Piracicaba Dental School, Department of Prosthodontics and Periodontology, Av. Limeira, 901, Piracicaba, São Paulo, Brazil, 13414-903*

[b] *Institute of Biomaterials, Tribocorrosion and Nanomedicine (IBTN)*

[c] São Paulo State University *(UNESP), Engineering College, Laboratory of Technological Plasmas, Av. Três de Março, 511, Sorocaba, São Paulo, Brazil, 18087-180*

[d] São Paulo State University (UNESP), Department of Physics, Av. Eng. Luís Edmundo C. Coube, 14-01, Bauru, São Paulo 17033-360, Brazil

[#] This article will be submitted on Applied Surface Science Journal.

Declarations of interest: none.

***** *Corresponding author.* Fax: +55-19-2106 5218.

E-mail address: vbarao@unicamp.br (V. Barão).

University of Campinas (UNICAMP), Piracicaba Dental School, Department of Prosthodontics and Periodontology, Av. Limeira, 901, Piracicaba, São Paulo, Brazil, 13414-903

ABSTRACT

We tailored different crystalline phases in sputtered TiO_2 films to verify their surface and electrochemical properties, protein adsorption, apatite layer formation and morphology on titanium-based implant material. Two TiO_2 crystalline phases (anatase and rutile) were grown on commercially pure titanium (cpTi) by magnetron sputtering to obtain the following groups: A-TiO_2 (anatase), M-TiO_2 (anatase and rutile mixture), R-TiO_2 (rutile). Non-treated cpTi was used as control. Surfaces were characterized as chemical composition, topography, crystalline phase and surface free energy (SFE). Electrochemical tests were conducted using simulated body fluid (SBF). Albumin adsorption was measured by bicinchoninic acid method. Hydroxyapatite (HA) precipitation was evaluated after 28 days of immersion in SBF. Sputtering treatment modified the topography of cpTi, increasing the surface roughness. CpTi and M-TiO_2 groups presented the greatest SFE. In general, TiO_2 crystalline phases showed improved electrochemical behavior, specially M-TiO_2 that showed the highest polarization resistance. Rutile phase exhibited a greater influence on decreasing the current density and corrosion rate, while the presence of a bi-phasic polycrystalline condition displayed a more stable passive behavior. Regarding protein interaction, M-TiO_2 increased albumin adsorption. The morphology of HA was dependent to the crystalline phase, being more evident in the bi-phasic group. The combination of anatase and rutile structures to generate TiO_2 films seems to be more suitable for biomedical implants application as greater corrosion protection, higher protein adsorption and bioactivity were accounted.

Keywords: Titanium; dental implants**;** corrosion**;** blood proteins; hydroxyapatites.

Highlights

- TiO_2 incorporation influenced the topography, roughness and surface free energy.
- Pure rutile phase and bi-phasic anatase and rutile trigger improved electrochemical stability.
- Bi-phasic polycrystalline TiO_2 enhances protein absorption.
- Different morphologies of hydroxyapatite are observed among TiO_2 phases.

1. Introduction

Biomedical implants have been widely used in actual and past years. The most used material is titanium (Ti) and its alloys due to their suitable properties such as excellent mechanical characteristics and superior biocompatibility compared to other alloys [1]. The excellent biocompatibility of Ti is due to the amorphous titanium dioxide (TiO_2) film naturally formed on its surface with a few nanometer (5–6 nm) thick [2], which protects Ti from body fluids attack, reducing ions release [3].

Even presenting this protective oxide layer, when exposed to body fluids, Ti is not able to prevent long term corrosion [2]. The corrosion process involves the release of metal ions and degradation products to surrounding tissue [4,5], which can result in adverse effects on the body (e.g. osteolysis, bone resorption, infections) and implants (e.g. loosening and failure) [2,4]. The thicker, more compact and stable the oxide layer, the better the corrosion resistance of an implant [6,7]. Thus, one strategy to improve Ti corrosion resistance could be the incorporation of a stronger TiO_2 film on Ti surface [3]. For instance, a thicker crystalline layer of TiO_2 (100 nm) on Ti surface significantly increases its corrosion resistance [8].

TiO_2 has a polymorphic nature [9], exhibiting two main crystalline phases: anatase and rutile.

Anatase exhibits a higher electron mobility and photocatalytic activity while rutile is the most stable phase at all temperatures and pressures, besides to present higher hardness [10,11]. Several methods can be used to create TiO_2 films including sol–gel [8,12], spin-coating [13], anodization [14,15], and magnetron sputtering [11,16,17]. Magnetron sputtering is widely used because it produces films with greater adhesion to the substrate, improved hardness and have a low cost of production [9,17–19]. Utmost important, this technique has the ability to generate pure TiO_2 phases of anatase and rutile [20].

The incorporation of TiO_2 into implants confers structural and functional benefits [11,21], being a useful material in the biomedical field due to its non-toxicity and non-inflammatory properties [22]. Additionally, TiO_2 powder presented a positive interaction with albumin, one of the most abundant human plasma proteins [23]. Protein adsorption is a key issue in the biocompatibility of medical implants [22] and it is considered the first major event induced on

the surface of the biomaterial when in contact with blood [12,24–26]. The initially adsorbed proteins cover the implant surface, leaving the surface appropriate for cell adhesion [27], and consequently integrating the implant to the tissues. Another key factor for implants material is the ability to form apatite [28] since it may dictate whether the material is able to bind to the living bone [29], which is extremely important to accomplish its osseointegration. Moreover, the shape and size of hydroxyapatite particles can stimulate inflammatory responses following implantation [21].

Thereby, it is evident that TiO_2 films may play an important role on several crucial factors for osseointegration process and implant treatment success. However, there is still no consensus in literature about which TiO_2 crystalline phase would be the most promising for biomedical applications, considering sputtering technique. Thus, here we tailored different crystalline phases in sputtered TiO_2 films to verify their surface and electrochemical properties, protein adsorption, apatite layer formation and morphology on Ti-based implant material.

2. Materials and methods

2.1 Experimental design

Commercially pure titanium (cpTi) discs with 10 mm in diameter and 1 mm thickness were polished, randomly divided and submitted to TiO_2 deposition treatment by radiofrequency (RF) magnetron sputtering. Different TiO_2 crystalline phases were deposited on the experimental groups: anatase (A-TiO_2), rutile (R-TiO_2) or mixture of phases (anatase + rutile) (M-TiO_2). Non-treated surface was considered the control group (cpTi). Surface analysis of crystalline phase, topography, chemical composition, and surface free energy were performed. The corrosion resistance of each surface was evaluated using standard electrochemical tests. Plasma protein interaction with the different surfaces were evaluated using albumin protein adsorption measurement. The surface ability to form apatite was evaluated using simulated body fluid (SBF). The experimental design is shown in Figure 1.

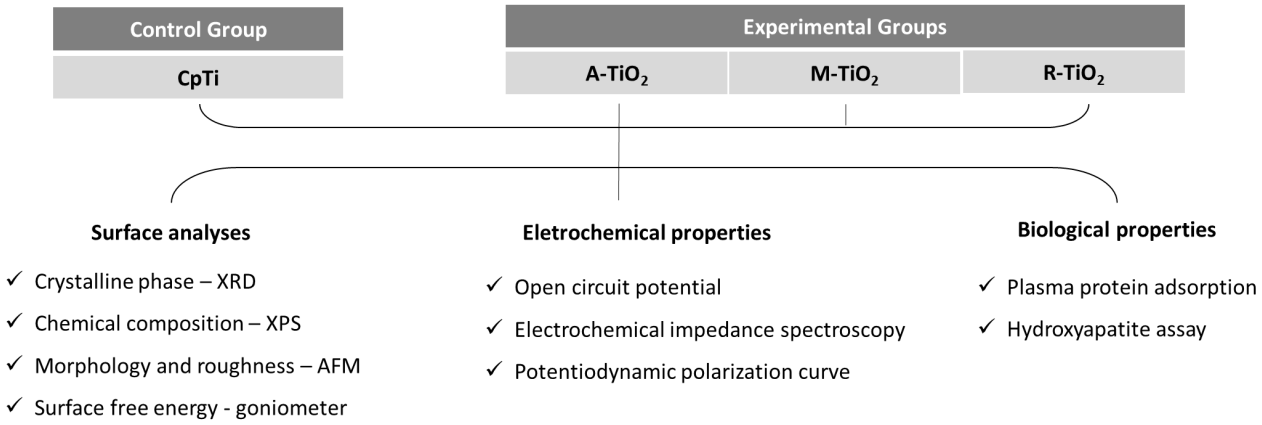

Figure 1. Experimental design of the study. XRD = X-ray diffraction, XPS = X-ray photoelectron spectroscopy, AFM = atomic force microscopy, cpTi = commercially pure titanium, A-TiO_2 = cpTi treated with pure anatase TiO_2 film, M-TiO_2 = cpTi treated with mixture of anatase and rutile TiO_2 film, R-TiO_2 = cpTi treated with pure rutile TiO_2 film.

2.2 Sample preparation

2.2.1 Polishing and cleaning procedures: CpTi discs were polished in an automatic polisher (EcoMet 300 Pro with AutoMet 250; Buehler, Lake Bluff, IL, USA) using sequential SiC grinding papers #320, #400 and #600 (Carbimet 2, Buehler). A mirror-finished surface was obtained with diamond paste (MetaDi 9- micron, Buehler) and colloidal silica polishing suspension (MasterMed, Buehler). Samples were ultrasonically cleaned in deionized water (10 min) and 70% propanol (10 min) (Sigma-Aldrich) and hot air dried [30].

2.2.2 Crystalline TiO_2 film deposition

TiO_2 film deposition was performed by a RF magnetron sputtering in a Kurt J. Lesker sputtering chamber (model KJL—System I) using a Ti-metal target (purity of 99.999%) (AJA International, North Scituate, MA, USA). Before each deposition, the target was sputtered with Ar for 10 min to ensure that the target was cleaned at the moment of the film growth [31]. The parameters used were previously reported by our group [11]. Sputtered samples were individually stored on dust free small bags before the surface and electrochemical analyses.

2.3. Surface analyses

2.3.1 Chemical composition and crystalline phase

The chemical composition of the surfaces was analyzed by X-ray photoelectron spectroscopy (XPS) (K-Alpha X-ray XPS, Thermo Scientific, Vantaa, Finland) using an Al K Alpha source, energy step size of 0.100 eV and a spot size of 400 μm (n = 1). Crystalline phase was verified using a X-ray diffraction (XRD) (Rigaku-Ultima 2000+, Rigaku Corporation, Salem, NH, USA) employing a Cu-K - λ = 1.54056 Å in a radiation operating at 40 kV and 20 mA at a continuous speed of 0.02° per second in a fixed angle 2.5° and a scan range from 15° to 80° (n = 1). XRD analysis was performed to confirm the TiO_2 incorporation and its crystalline phases.

2.3.2 Morphology and topography

The morphology and topography of the surfaces were observed by atomic force microscopy (AFM) (Park System-NX-10; Park systems, Suwon, Korea) in a tapping mode with a constant force of 42 N/m, using a frequency of 320 kHz. Two- and three-dimensional micrographs of 20 × 20 μm, 5 × 5 μm and 1 × 1 μm were obtained (n = 1). Values of roughness arithmetic average (Ra) and root means square average (RMS) were obtained in three different areas of the 20 × 20 μm micrograph, and the total surface area was estimated using specific software (Gwyddion v 2.37; GNU General Public License; Czech Republic).

2.3.3 Surface free energy

Surface free energy (SFE) was evaluated using a goniometer (Ramé-Hart 100-00; Ramé-Hart Instrument Co., Succasunna, NJ, USA) by the sessile drop (2 mL) method through the Owens–Wendt approach (n = 5). Polar (water) and dispersive (diiodomethane) components were used to determine the SFE, considering the contact angle formed in the surfaces by liquids with different polarities. Measurement of contact angles was conducted by the Ramé-Hart DROP image Standard software (Ramé-Hart 100-00; Ramé-Hart Instrument Co.) [32].

2.4 Electrochemical properties

The electrochemical behavior of cpTi, A-TiO_2, M-TiO_2 and R-TiO_2 surfaces (n = 5) was evaluated in simulated body fluid (SBF; pH 7.4; 37 ±1 ºC) [30,33] based into the regulatory standards of

the ASTM International (formerly the American Society for Testing and Materials – ASTM) (G61–86 and G31–72). The electrochemical tests were conducted as per our previous protocol [33]. Briefly, three tests were conducted: open circuit potential (OCP), electrochemical impedance spectroscopy (EIS) and potentiodynamic polarization curve were performed using a three-electrode cells associated with a potentiostat (Interface 1000, Gamry Instruments, Warminster, PA, USA). A saturated calomel electrode (SCE) was used as a reference electrode and a graphite rod as a counter electrode. For data analyses, the exposed area of 0.79 cm^2 was considered for all surfaces (working electrode). EIS data were examined by Echem Analyst software (Gamry Instruments) using an appropriated circuit for each surface to determine the polarization resistance (R_p) and capacitance (Q) of the oxide layer. Nyquist, Bode, and phase angle plots were drawn. The potentiodynamic polarization curves were analyzed by the Tafel extrapolation method (Echem Analyst Software, Gamry Instruments) to obtain the following parameters: E_{corr} (corrosion potential), i_{corr} (corrosion current density), i_{pass} (passivation current density) and corrosion rate.

2.5. Biological properties

2.5.1 Plasma protein adsorption

To evaluate the plasma protein interaction with TiO_2 surfaces, albumin adsorption was investigated. Five samples of each group were incubated in 100 mg/mL of albumin (Sigma–Aldrich, St. Louis, MO, USA) under horizontal stirring (7.85 rad/s) at 37 °C for 2 h. After incubation, in order to remove non-adherent proteins, samples were washed twice in phosphate-buffered saline (PBS) (Gibco, Life Technologies, Gaithersburg, MD, USA) and transferred to cryogenic tubes containing 1 mL of PBS. Samples were sonicated at an amplitude of 80% for 60 s. The solution was vortexed and 10-fold serially diluted. Finally, the protein adsorption was evaluated by the bicinchoninic acid method (BCA Kit, Sigma–Aldrich, St. Louis, MO, USA), following the manufacturer's recommendation. The protein adsorption was calculated according to a standard curve prepared with bovine serum albumin [33,34].

2.5.2 Hydroxyapatite precipitation

In order to investigate the bioactivity of the surfaces, samples were immersed in SBF solution, which has concentration and composition similar to the human body fluid [35]. SBF solution was prepared according to a previous protocol [29]. Control and experimental discs were soaked in polypropylene tubes with 7.9 mL of SBF and incubated at 37 °C for 28 days. SBF was refreshed every 24 h. After soaking for 28 days, samples were gently washed in purified water and dried in a desiccator without heating [29]. To observe hydroxyapatite precipitation, samples were analyzed by scanning electron microscopy (JEOL JSM 5600 PV, JEOL, Tokyo, Japan) at 15 kV in magnifications of 500×, 1000×, 2000× and 8000×.

2.6 Statistical analyses

One-way ANOVA was used to test the influence of different surface conditions (4 levels) on the SFE, electrochemical parameters and protein adsorption. Tukey HSD test was used as a post-hoc technique to compare groups. A mean difference significant at the 0.05 level was used for all tests (IBM SPSS Statistics for Windows, v. 21.0., IBM Corp., Armonk, NY, USA).

3. Results

3.1 Surface properties is dependent on the TiO_2 crystalline phase

The chemical composition of the outer layer formed on the surfaces was analyzed using XPS. All surfaces were chemically composed of titanium (Ti), oxygen (O) and carbon (C) (Figure 2a). Considering C is a contaminant, it was excluded from the analysis [36]. The detailed spectra of peaks and the atomic percentage of each compound are presented. Two peaks of Ti were observed in the Ti 2p binding energy region in all surfaces, Ti 2p1/2 and Ti 2p3/2 located at 464.7 eV and 458.4 eV respectively (Figure 2b). The energy difference between the peaks of Ti 2p1/2 and Ti 2p3/2 is 5.7 eV, thus it is expected to be Ti^{4+} in TiO_2 bond [2]. A TiO_2 bind can be observed at 530 eV on the oxygen spectrum, and the peak at 532 eV is related to O–H hydroxyl species and the peak correlated to C–O, which represent contaminants. Considering the presence and localization of the referred peaks, it suggests the binding of Ti and O, configuring

the TiO_2. The A-TiO_2 spectrum presented a slight shift of the peaks compared to the other groups. This shift can be probably due to the less oxygen content on this surface.

The surface crystallinity was analyzed by XRD (Figure 2c). All the diffraction peaks found were related to titanium and its oxide phases. Titanium peaks were found in all surfaces due to the substrate being made of titanium. TiO_2 peaks such as anatase and rutile were found only in TiO_2 coated surfaces at 25 and 27 (2θ) respectively. The A-TiO_2 surface showed anatase and titanium peaks, M-TiO_2 presented titanium and a mixture of anatase and rutile peaks, while R-TiO_2 was composed of rutile and titanium peaks. It suggests that the TiO_2 films were successfully grown, since the films present different crystalline phases as proposed.

a)

	XPS atomic concentration (%)		
Groups	**Ti2p**	**O1s**	**C1s**
cpTi	11.94	42.57	45.49
A-TiO_2	8.67	27.00	64.33
M-TiO_2	10.35	33.73	55.92
R-TiO_2	11.35	33.6	55.05

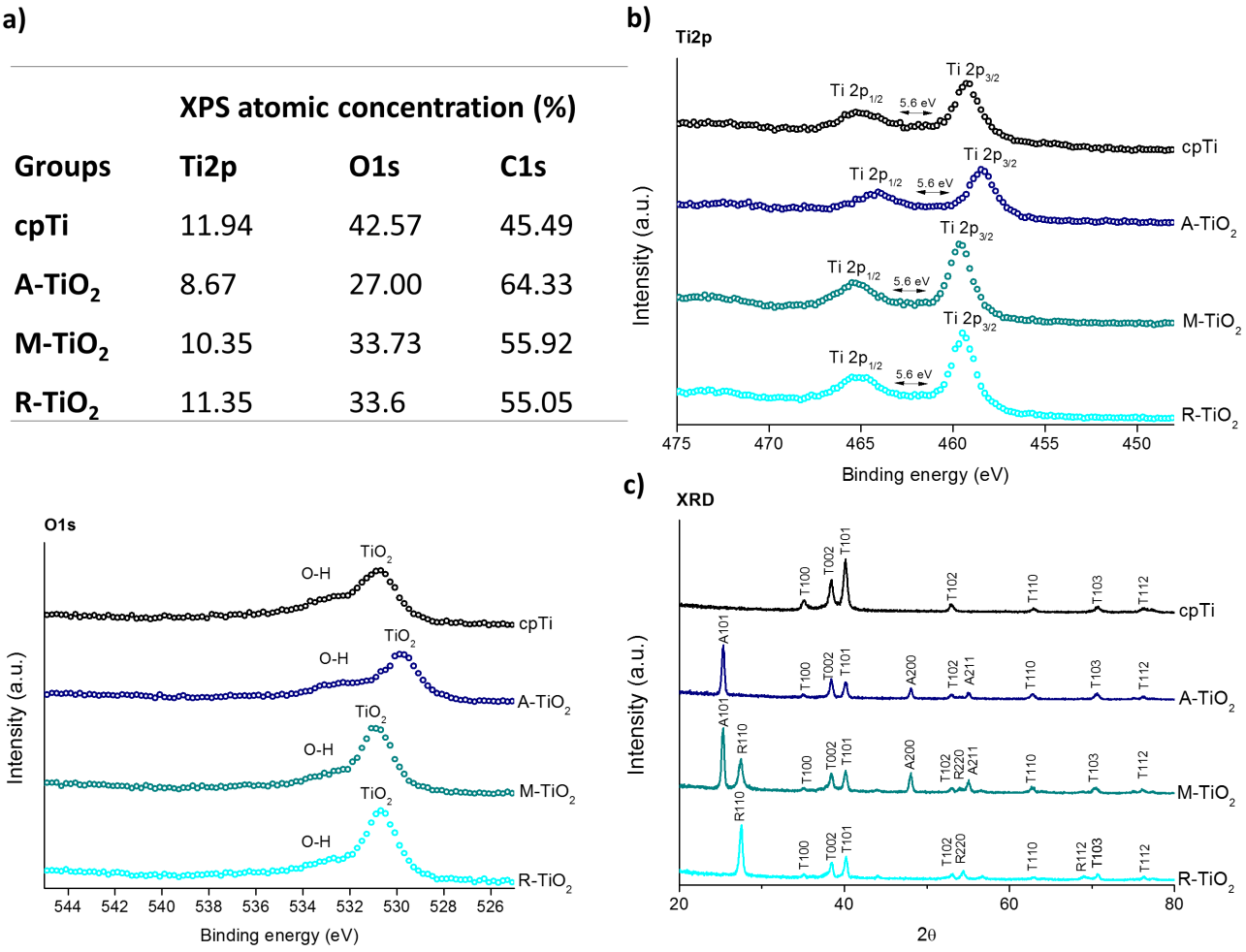

Figure 2. (a) Atomic concentration (%) composition of cpTi, A-TiO_2, M-TiO_2 and R-TiO_2 surfaces obtained by XPS (n = 1). **(b)** Detailed XPS spectra for Ti2p and O1s and **(c)** XRD pattern of cpTi,

A-TiO_2, M-TiO_2 and R-TiO_2 surfaces (n = 1). Letters T, A and R in the XRD plot refers to corresponding peaks of titanium, anatase and rutile, respectively.

The surface morphology and topography can be seen in Figure 3. CpTi surface presented a smoother surface compared to the TiO_2-treated groups as a result of its mirror-finished condition. TiO_2 groups showed a granular surface, suggesting TiO_2 nanoparticles incorporation, and presented homogenous film distribution on the entire substrate. R-TiO_2 surface exhibited greater grains size than M-TiO_2 and A-TiO_2. A tridimensional profile illustrates the peaks and valleys obtained for each surface. TiO_2 mixture phase showed the highest values of Ra and RMS followed by rutile, anatase and cpTi, respectively.

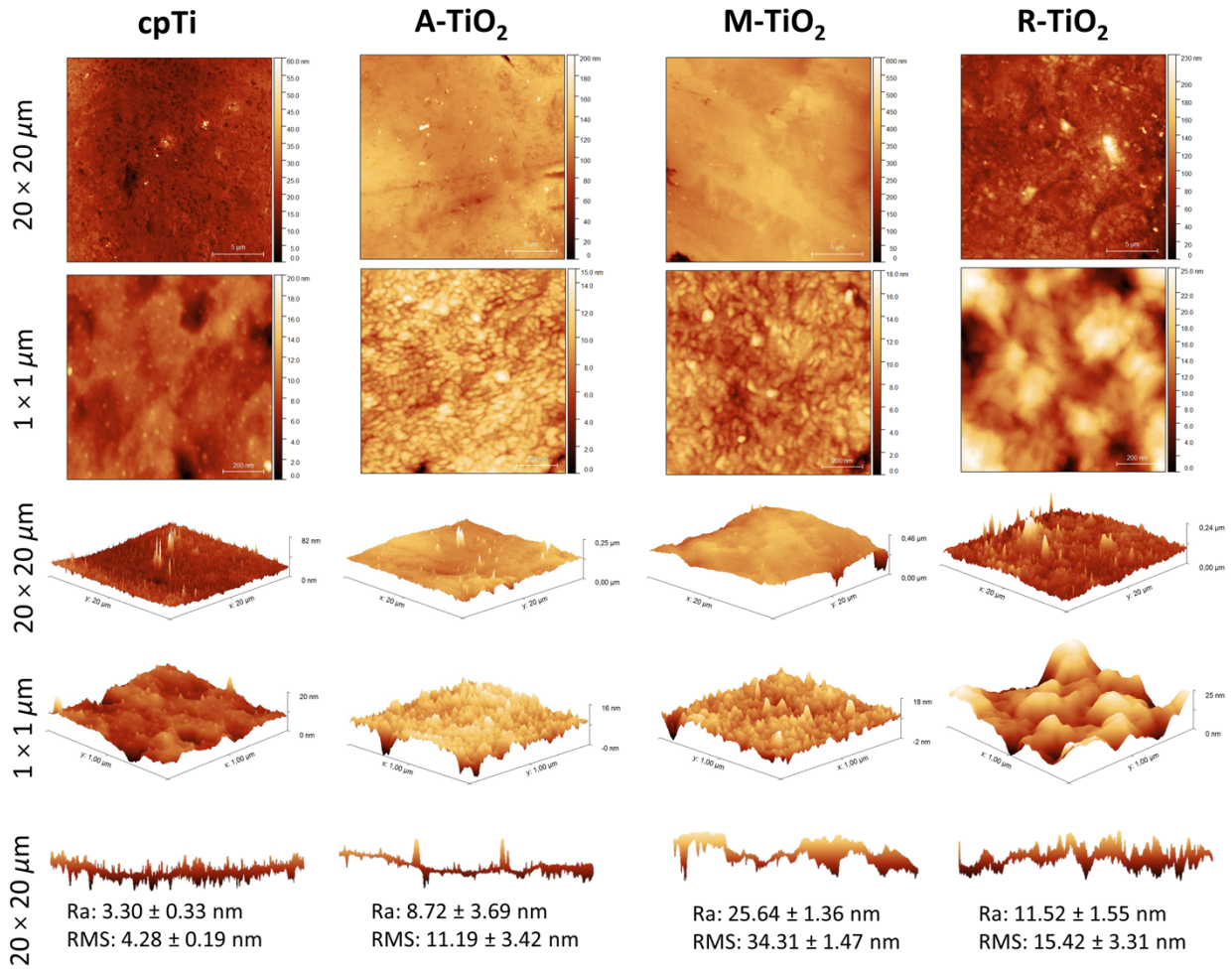

Figure 3. Topography, roughness average (Ra) and root means square (RMS) of cpTi, A-TiO_2, M-TiO_2 and R-TiO_2 surfaces obtained by AFM (n = 1).

Wettability is dependent on the SFE and contact angle data. SFE was calculated using the water and diiodomethane contact angles. The smaller the contact angle, the higher the SFE and wettability. SFE of each surface is shown in Figure 4a and their contact angles are shown in Figure 4b. Here is possible to see the affinity of each surface with dispersive and polar components. All surfaces presented a higher affinity with the polar component, which means that the water sessile drop presented a greater spread on the surfaces compared to the diiodomethane sessile drop. CpTi and mixture surfaces presented the highest SFE.

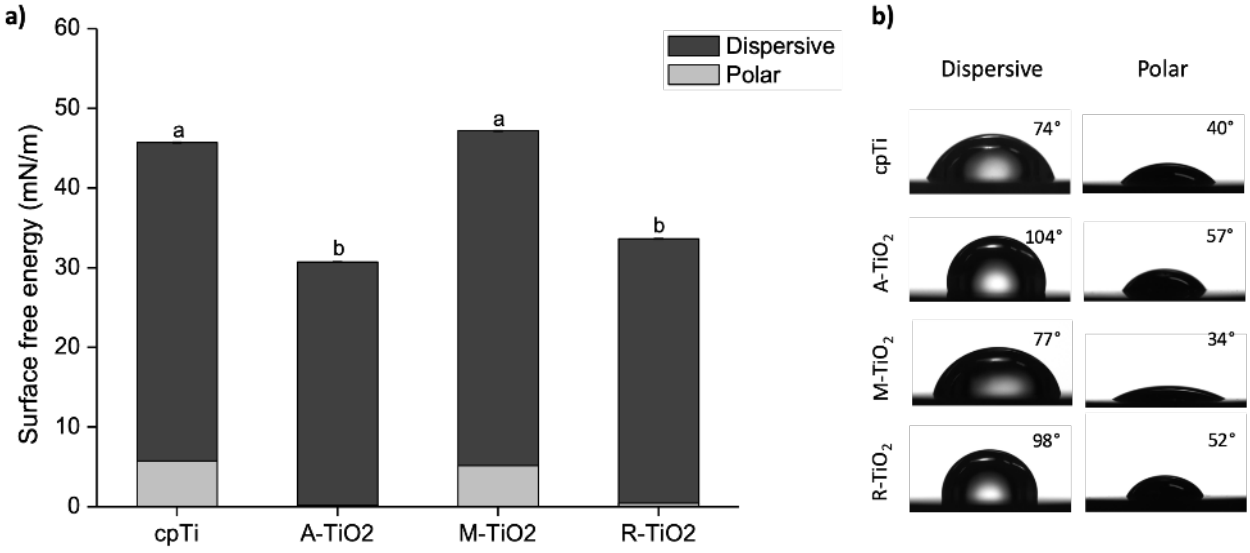

Figure 4. (a) Surface free energy and **(b)** contact angle of cpTi, A-TiO_2, M-TiO_2 and R-TiO_2 surfaces (n = 5). Different letters indicate statistically significant differences between groups ($p<0.05$, Tukey HSD test).

3.2 TiO_2 drives improved electrochemical stability

The oral environment plays an important role on long-term implant materials durability because of their interaction with body fluids. In this context, electrochemical tests were carried out to evaluate the corrosion resistance and stability of the TiO_2 film as a function of different crystalline phases. CpTi and TiO_2-treated surfaces were immersed in SBF to observe the OCP evolution (Figure 5) and the free potential of material for 1 h (Table 2). Although all surfaces presented a clear stable potential (vs. SCE) after immersion in SBF, R-TiO_2 and M-TiO_2 tended to

faster stabilize the potential (around 250 s after immersion) than the other groups. This behavior can be related to a rapidly growth of a spontaneous passive film on the materials surface. Interestingly, A-TiO_2 showed the most electropositive potential, which is indicative of a nobler behavior.

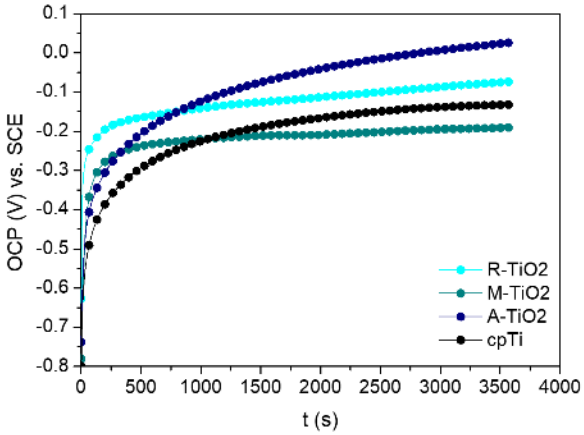

Figure 5. Representative open circuit potential evolution (vs. SCE) curves of cpTi, A-TiO_2, M-TiO_2 and R-TiO_2 surfaces as a function of time in SBF.

Table 2. Mean (and standard deviation) of open circuit potential (OCP) (vs. SCE) of cpTi, A-TiO_2, M-TiO_2 and R-TiO_2 surfaces (n = 5) after 1 h in SBF.

Group	OCP (V vs. SCE)
cpTi	-0.13 (0.06)^{bc}
R-TiO_2	-0.07 (0.02)^{b}
M-TiO_2	-0.19 (0.01)^{c}
A-TiO_2	0.02 (0.01)^{a}

Different letters indicate statistically significant differences between groups ($p<0.05$, Tukey HSD test).

EIS assessment was performed to understand the electric properties of the film/oxide layer formed on each surface. Wider diameter for the hemiarches of Nyquist plots (Figure 6a) and higher values of impedance (|Z|) and phase angle on the bode plot (Figure 6b) represent a more protective behavior against corrosion. TiO_2 film improved the electrochemical stability of Ti where M-TiO_2 displayed the most open hemiarch followed by the R-TiO_2 (Figure 6a). Both

groups also exhibited higher values of impedance (Figure 6b). Analyzing the phase angle, two-time constants are clearly seen for M-TiO_2 and A-TiO_2 but with different shapes. While the surface formed only with anatase phase presented higher phase angle at higher frequencies, the mixture-phase group showed a considerable increase for this parameter at low frequencies, which can imply in a greater resistance to corrosion of the inner regions of the film. On the other hand, R-TiO_2 demonstrated the best performance at low frequencies with a very stable phase angle for the intermediate frequencies.

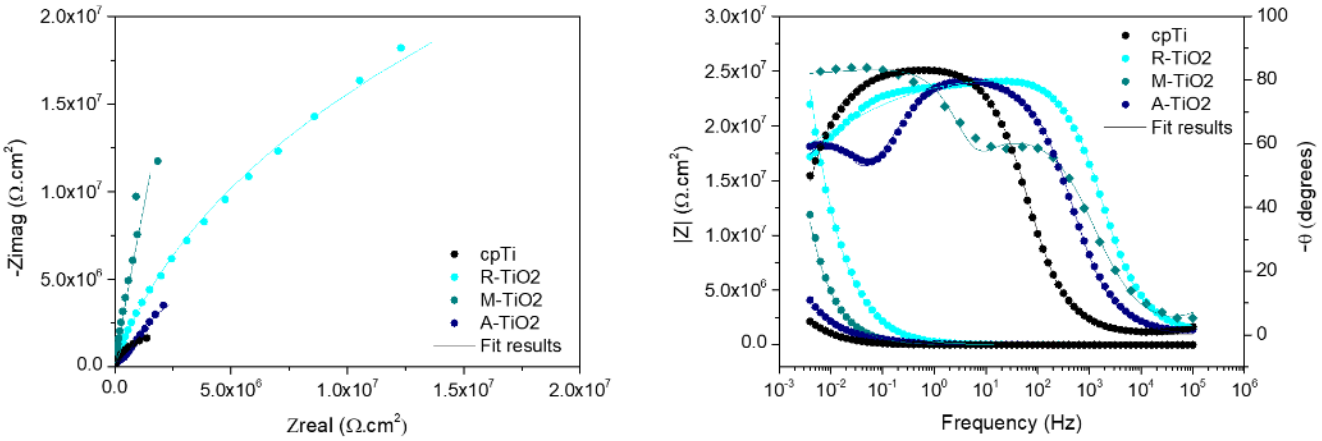

Figure 6. (a) Representative Nyquist and **(b)** bode plots of cpTi, A-TiO_2, M-TiO_2 and R-TiO_2 surfaces.

The electrochemical parameters (Table 3) were obtained after fitting the EIS results with equivalent circuits (Figure 7). CpTi group was fitted with a simple circuit consisting of R_p (polarization resistance) and a constant phase element (CPE, named as Q) in parallel (Figure 7a). For the TiO_2-treated groups, another pair of elements was considered due to the presence of the film; hence two different electrochemical interfaces are presented. The external and internal electrochemical interfaces were represented by Q_{out}/R_{pout} and Q_{in}/R_{pin}, respectively (Figure 7b). To confirm if the EIS data were appropriately fitted, the fitting lines are shown in the Nyquist and bode plots. Additionally, the chi-square (χ^2) values for all groups were settled in the order of 10^{-3} (Table 3), showing that the equivalent circuit chosen for each surface is adequate. Q_{tot} and R_{ptot} were obtained by the sum of both Q and R_p and used for the statistical analysis. The polarization resistance of M-TiO_2 was more than 3 orders higher compared with

other groups ($p < 0.05$). On the other hand, R-TiO_2 possessed the lowest values of capacitance. In fact, all the TiO_2-treated surfaces showed statistical lower Q_{tot} than control cpTi ($p < 0.01$), evidencing their protective behavior. For all TiO_2 films, the R_{pin} was higher than R_{pout}. However, A-TiO_2 showed a higher Q for the inner electrochemical interface, which can infer a decrease of the corrosion resistance. This fact can be related with the drop of the phase angle in low frequencies. M-TiO_2 seems to be the most homogeneous film since it had the highest η values for both electrochemical interfaces.

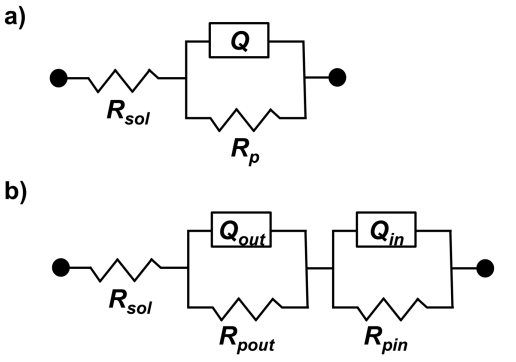

Figure 7. Equivalent circuits used to fit EIS data of **(a)** cpTi, **(b)** A-TiO_2, M-TiO_2 and R-TiO_2 surfaces. R_{sol} represents the solution resistance; Q represents the constant phase element of a sigle compact oxide layer; Q_{out} and Q_{in} represent the constant phase element of the outer and inner oxide layer, respectively; and R_{pout} and R_{pin} represent the polarization resistance of the outer and inner oxide layer, respectively.

Table 3. Means (standard deviations) of electrical parameters obtained from the equivalent circuit models of cpTi, A-TiO_2, M-TiO_2 and R-TiO_2 surfaces (n = 5).

Groups	R_{pout} ($M\Omega \cdot cm^2$)	R_{pin} ($G\Omega \cdot cm^2$)	Rp_{tot} ($G\Omega \cdot cm^2$)	Q_{out} ($S*s^{a} \cdot cm^{-2}$)$\times 10^{-6}$	η_{out}	Q_{in} ($S*s^{a} \cdot cm^{-2}$)$\times 10^{-6}$	η_{in}	Q_{tot} ($S*s^{a} \cdot cm^{-2}$)$\times 10^{-6}$	$\chi^2 \times 10^{-3}$
cpTi	3.75 (0.81)		3.75×10^{-3} (0.81×10^{-3})[b]	10.28 (0.65)	0.94 (0.01)			10.28 (0.65)[a]	1.30 (0.86)
R-TiO_2	5.75 (9.95)	2.51 (3.90)	2.51 (3.89)[b]	0.46 (0.08)	0.92 (0.02)	0.18 (0.07)	0.49 (0.13)	0.64 (0.16)[d]	0.78 (0.56)
M-TiO_2	0.02 (0.01)	3259.59 (2815.91)	3262.68 (2818.58)[a]	1.48 (0.03)	0.84 (0.01)	1.34 (0.11)	0.97 (0.01)	2.82 (0.20)[c]	4.65 (0.50)
A-TiO_2	0.45 (0.46)	0.02 (0.01)	0.02 (0.01)[b]	2.15 (0.11)	0.91 (0.01)	3.85 (0.55)	0.78 (0.01)	6.00 (0.98)[b]	0.47 (0.09)

Different letters indicate statistically significant differences between groups ($p<0.05$, Tukey HSD test).

The electrochemical stability of TiO_2 films was also tested based on variety of cathodic and anodic potentials via potentiodynamic polarization test. A representative polarization curve for each group is shown in Figure 8 and the electrochemical parameters derived from these curves are described in Table 4. R-TiO_2 and M-TiO_2 exhibited the greatest corrosion behavior, where nobler E_{corr} values and lower i_{corr}, i_{pass} and corrosion rate were noted ($p < 0.05$). However, observing the polarization curves some differences may be noticed. For instance, the film composed by the mixture of anatase and rutile displayed a remarkable passive behavior. It can be observed by a stable and wider passivation region at very low current density that starts almost immediately after the onset of the anodic region. The presence of the film seems to influence this feature, since all TiO_2-treated groups showed the passivation region shifted to the left of the graph.

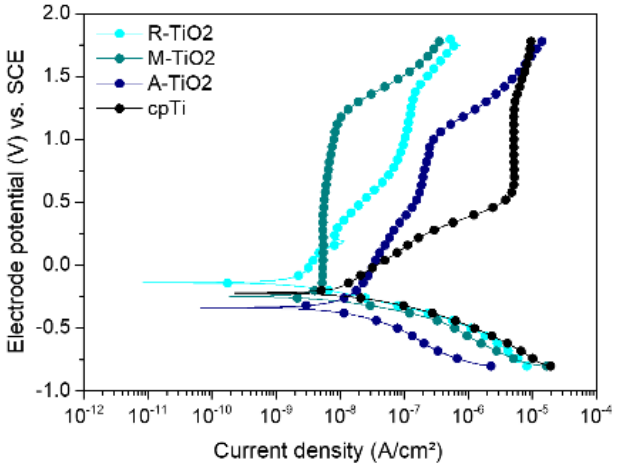

Figure 8. Representative polarization curves of cpTi, A-TiO_2, M-TiO_2 and R-TiO_2 surfaces.

Table 4. Mean and (standard deviation) values of electrochemical parameters obtained from the potentiodynamic polarization curves of cpTi, A-TiO_2, M-TiO_2 and R-TiO_2 surfaces (n=5).

Group	E_{corr} (mV) vs. SCE	i_{corr} (nA)	i_{pass} (nA)	Corrosion Rate (mpy) × 10^{-3}
cpTi	-285.20 (100.86)^{b}	9.08 (1.38)^{b}	4593.42 (350.92)^{a}	4.15 (0.63)^{b}
R-TiO_2	-125.00 (44.91)^{a}	2.68 (1.07)^{c}	8.22 (1.44)^{b}	1.22 (0.39)^{c}
M-TiO_2	-238.75 (24.90)^{ab}	3.61 (0.42)^{c}	5.73 (0.66)^{b}	1.65 (0.15)^{c}
A-TiO_2	-324.75 (19.21)^{b}	16.01 (2.75)^{a}	25.20 (2.41)^{b}	7.31 (0.98)^{a}

Different letters indicate statistically significant differences between groups ($p<0.05$, Tukey's HSD test).

3.3 Protein adsorption and apatite morphology are surface dependent

Figure 9 displays the interaction between cpTi and TiO_2-treated surfaces with albumin. M-TiO_2 surface presented the highest albumin adsorption compared to the cpTi, A-TiO_2 and R-TiO_2 which presented a similar behavior. The association of higher surface roughness and surface free energy may be one reason for this superiority.

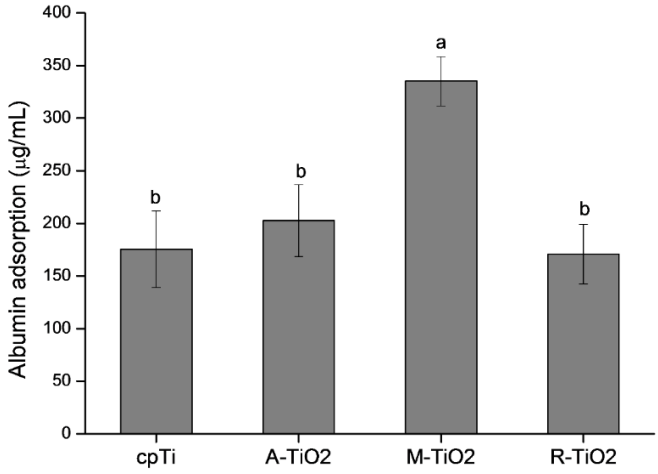

Figure 9. Albumin adsorption of cpTi, A-TiO_2, M-TiO_2 and R-TiO_2 surfaces (n = 5). Different letters indicate statistically significant differences between groups ($p<0.05$, Tukey HSD test).

The hydroxyapatite layer formed on the surfaces after immersion in SBF solution for 28 days are shown in Figure 10. All surfaces were able to form apatite; however, the apatite morphology was surface dependent. CpTi and A-TiO_2 presented a needle shaped morphology whereas M-TiO_2 and R-TiO_2 presented a spherical shaped, in which a considerable small feature for M-TiO_2 can be observed. The hydroxyapatite layer formation over TiO_2 surfaces containing rutile were more complete compared to the cpTi surface and A-TiO_2, which presented only agglomerates on their surface.

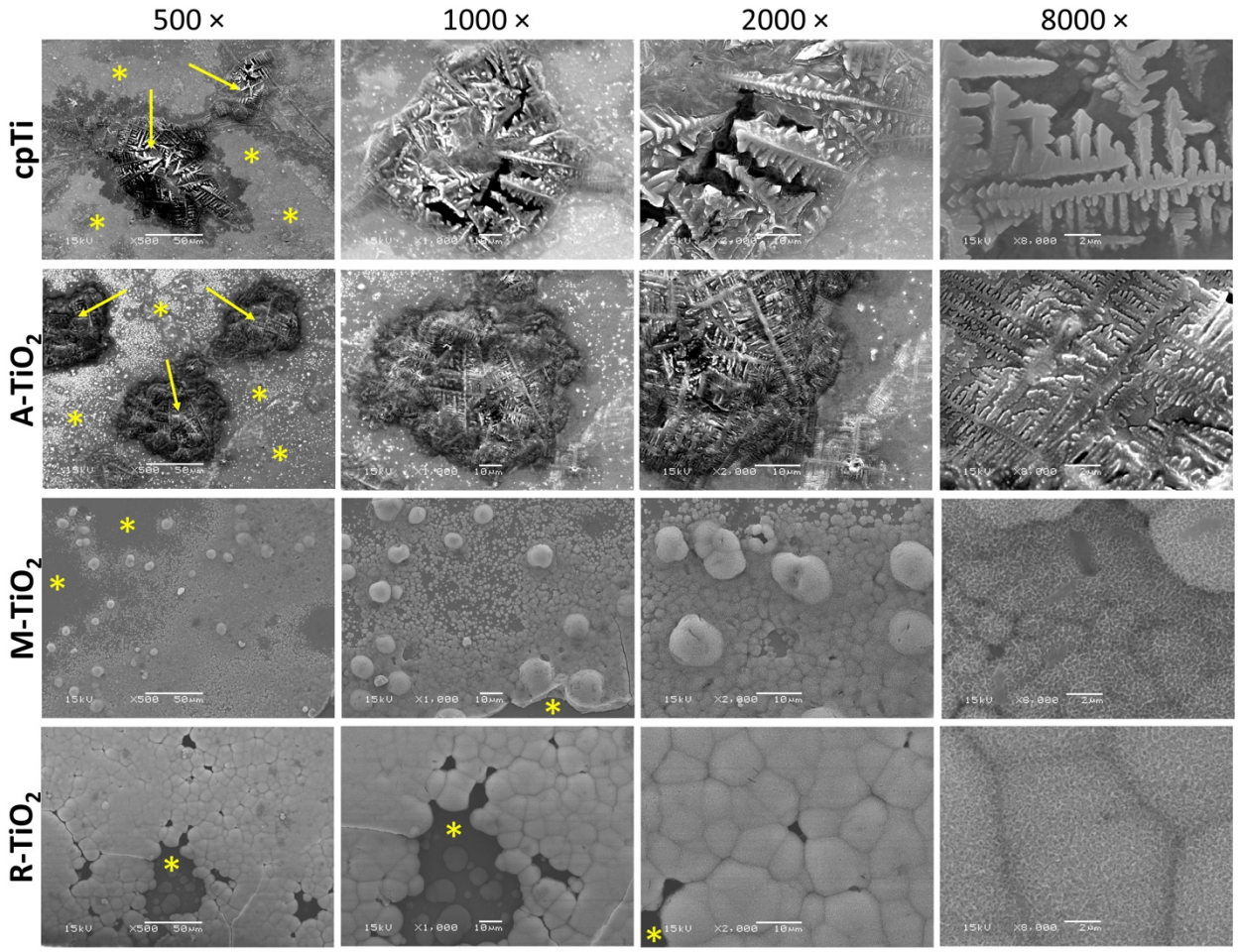

Figure 10. Scanning electron micrographs (at 15 kV) of hydroxyapatite layer on cpTi, A-TiO_2, M-TiO_2 and R-TiO_2 surfaces immersed in SBF after 28 days. Scale bar = 10 μm. (Arrows indicates hydroxyapatite precipitation and * indicates uncovered surface.

4. Discussion

Developing protective and bioactive films for biomedical implants has been shown an important option to ensure treatment success in the last years. Herein, TiO_2 films with different crystalline phases (anatase, rutile and a mixture of phases) were incorporated onto cpTi surfaces. These films (312-338 nm) [11] were able to improve the corrosion resistance and biological properties of this biomaterial. To the best of our knowledge, this is the first time that these features could be directly correlated with the crystalline phases of films formed by magnetron sputtering on cpTi. TiO_2 crystalline phases drove the surface properties, electrochemical parameters, albumin adsorption and hydroxyapatite precipitation.

Previews studies have demonstrated that TiO_2 films formed by sputtering are more stable than the natural oxide layer formed on metal surfaces, and can effectively enhance the corrosion resistance of Ti by reducing the cathodic and anodic reactions [37,38]. In general, M-TiO_2 and R-TiO_2 showed the best behavior for all electrochemical tests. Concerning to R-TiO_2, this surface presented the lowest values of Q_{tot}, i_{corr} and corrosion rate, which are parameters related with the ions exchange between the electrolyte and substrate. The lower these values, the higher the corrosion resistance. In this case, the film acted as a barrier against the transport of ionic species in the electrolyte through the surface slowing down the electrochemical process [37]. It is well known that rutile phase is the most stable, dense and resistant among the crystalline TiO_2 phases [10,39], which may have guaranteed the above-mentioned results.

Consonantly, M-TiO_2 surface must be highlighted since the mixture of anatase and rutile produced a surface with polarization resistance almost 6 orders higher than the non-treated control group, indicating an extreme protection against corrosion. Besides that, M-TiO_2 displayed a great passivation behavior which can ensure long-term electrochemical stability and lower degradation rates of the implant material. This behavior may be related to the higher degree of crystallinity [40] that was obtained by the combination of both TiO_2 phases. Besides, this surface may have a more homogeneous film with small or none defects/pores and a strong bonded interface with the substrate, which can be confirmed by the higher values of η_{in} and greatest phase angle at low frequencies, resulting in a drastic inhibition in pitting propagation [41]. The small Q_{tot} difference between M-TiO_2 and R-TiO_2 can be explained by the surface features, since the higher roughness and wettability of the mixture group may affect negatively the passive film formation [42,43] and can enhance the electrochemical exchanges by lowering the contact resistance between the electrode and electrolyte [43,44], respectively.

In contrast, A-TiO_2 exhibited the worst electrochemical performance among the sputtered surfaces, but still better than that of non-treated control. Some hypotheses can be drawn to such behavior. Firstly, A-TiO_2 film presented the most electropositive potential (OCP) amongst the surfaces exhibiting the highest difference with the cpTi. Such difference can favor the occurrence of galvanic corrosion between the coating and the substrate [37]. Secondly, the small amounts of Ti2p and O1s observed in the XPS analyses may be another

reason since Ti has a very high affinity towards O and their decrease can reflect in a low degree of crystallinity, and the presence of amorphous inclusions in the film structure [40]. In addition, among the TiO_2 surfaces, anatase has the lowest hardness [11] and may be less stable than the other films leading to an increase in the degradation rate. Thus, it is notable that rutile phase presents a greater positive influence on the electrochemical stability of films formed on Ti. However, the combination of both TiO_2 phases showed a remarkable protective behavior. Controlling the amount of rutile in M-TiO_2 films could be a way to improve even more this surface since it seems that a higher amount of anatase is observed over rutile in the XRD spectra.

With regard to the morphology found in the studied surfaces, it was quite characteristic of TiO_2 nanoparticles incorporation, since TiO_2 nanoparticles are smaller than 1 μm and are used to arrange in agglomerates [10]. The particle size varied according to the crystalline phase [45]. Rutile presented larger grains compared to small anatase grains, and it is possible to note grains of both sizes in the mixture surface, which may justify its greater roughness. The difference in the grain size is due to the crystallinity process, in which amorphous TiO_2 firstly forms anatase, which can be transformed in rutile phase. The rutile particle shape suggests that its grains has formed via the coalescence of several “prior” anatase particles [46], increasing the grain size and reducing the surface area [45].

Correlating surface morphology and contact angle, it is known that surface roughness can directly influence the contact angle. The highest roughness observed on mixture phase reflected on its higher hydrophilicity status, which can be explained by the Wenzel state, in which the liquid is in contact with the asperities of the surface [47,48]. However, for A-TiO_2 and R-TiO_2 surfaces it was different, since they presented the lowest roughness and a similar contact angle to the mixed phase group. Such behavior can be explained by the Cassie−Baxter relation, in which the droplet sits on top of the roughened surface with trapped air underneath, presenting a reduced spreading and consequently an increasing in its contact angle [47,48].

Furthermore, roughness and surface free energy can influence the protein adsorption [49,50]. While higher roughness may enhance the number of binding sites for proteins, a superior surface free energy can lead to an improved interaction between fluids and surface. The mixture of anatase and rutile phases presented the greatest albumin adsorption, which

can be explained by its higher roughness and surface free energy compared to the other surfaces. Both anatase [12,22] and rutile [2] separately are capable of adsorbing proteins on their surfaces. A previous study also investigated the albumin adsorption onto mixture of anatase and rutile using the TiO_2 powder P25, varying the ionic strength and pH, and found that albumin adsorption was achieved within a few minutes [51]. It has been showed that the albumin adsorption among powders of anatase, rutile and the mixture of phases were similar [23]. As can be seen, herein all surfaces were able to interact with albumin. The film formed by the mixture phase of TiO_2 seems to be more interesting to albumin adsorption. The difference between our results and the literature is related to the material and evaluation method. The reported studies used TiO_2 powder dissolved in solutions to verify the protein adsorption, while in the present study we used a resistant TiO_2 film-bonded nanoparticles formed by a sputtering method that presents other features (e.g. roughness, wettability, composition) to be considered.

Despite anatase seems to be more favorable for the apatite formation [52], this study shows that all TiO_2 surfaces were able to form hydroxyapatite layer. Furthermore, the greater hydroxyapatite coverage in TiO_2 surfaces was previously described since TiO_2 seems to present higher bioactivity than the bare Ti substrate [52,53]. However, different hydroxyapatite morphologies were found between surfaces. It can be justified by the different surface morphologies of the studied groups. As a matter of fact, the groups presenting rutile seems to stimulate greater hydroxyapatite coverage and to modify its morphology. The differences in hydroxyapatite morphology can be justified by the presence of some points: (1) different surface topographies, since rough surface topography may lead to a more uniform hydroxyapatite coating than a smoother surface; and (2) the differences in matching between the crystal orientation of the initially formed hydroxyapatite crystals and the crystal directions of the substrate surface [53]. Seeing that anatase is the first crystal to be formed from Ti, it can justify the similarity of hydroxyapatite morphology between cpTi and A-TiO_2 surfaces. With regard to M-TiO_2 and R-TiO_2, it is clear that the hydroxyapatite spherical shaped have grown following the grain sizes of each surface with smaller spheroids for mixture group. As observed in AFM images, M-TiO_2 formed smaller grains than rutile alone. Furthermore, the morphology and particle size of hydroxyapatite seems to influence inflammatory response, being that needle-shaped hydroxyapatite generated a prolonged

inflammatory response compared to spherical shaped hydroxyapatite [21]. Notwithstanding, the cell viability seems to not be influenced by the different hydroxyapatite features, since human fibroblast cells presented similar viability to different hydroxyapatite morphologies synthesized in vitro [54]. Thus, in relation to hydroxyapatite precipitation, M-TiO_2 and R-TiO_2 seems to be more interesting for the osseointegration process.

In summary, this study grew films of pure anatase, pure rutile and a mixed of anatase and rutile TiO_2 crystalline phases onto Ti-based material to determine their electrochemical stability, protein adsorption and hydroxyapatite precipitation capacity. Considering our results, TiO_2 consistently improved electrochemical stability, protein adsorption and bioactivity of Ti surface, and among the three studied TiO_2 phases, the mixed TiO_2 is the most promising surface for implant applications. Extrapolating to a clinical situation, it is possible to infer that the mixed TiO_2 film can enhance the longevity and success of biomedical implant treatment.

5. Conclusions

TiO_2 films presenting different crystalline phases (anatase, rutile and mixture phases) were grown on titanium substrates using magnetron sputtering. The role of each TiO_2 phase on the surface properties, electrochemical stability, protein adsorption and apatite formation were outlined to define the most suitable option to sputter titanium surfaces for biomedical implant applications. Herein, phase pure rutile TiO_2 and bi-phasic rutile and anatase TiO_2 films trigger superior electrochemical stability. However, the bi-phasic TiO_2 film seems to be more promising for implants application as greater albumin adsorption and bioactivity are noted.

Declarations of interest

None.

Acknowledgments

This work was supported by the Brazilian National Council for Scientific and Technological Development (CNPq) (grant number 136602/2017-7) and by the São Paulo State Research Foundation (FAPESP), Brazil (grant number 2015/17055-8 and 2016/11470-6). Authors also

express their gratitude to the Brazilian Nanotechnology National Laboratory (LNNano) at the Brazilian Center of Research in Energy and Materials (CNPEM) for the AFM and XPS facilities.

References

[1] M. Kulkarni, A. Flasker, M. Lokar, K. Mrak-Poljšak, A. Mazare, A. Artenjak, S. Cucnik, S. Kralj, A. Velikonja, V. Kralj-Iglic, S. Sodin-Semrl, P. Schmuki, A. Iglič, Binding of plasma proteins to titanium dioxide nanotubes with different diameters, Int. J. Nanomedicine. 10 (2015) 1359. https://doi.org/10.2147/IJN.S77492.

[2] E.S. Bronze-Uhle, L.F.G. Dias, L.D. Trino, A.A. Matos, R.C. de Oliveira, P.N. Lisboa-Filho, Physicochemical characterization of albumin immobilized on different TiO2 surfaces for use in implant materials, Colloids Surfaces A Physicochem. Eng. Asp. 564 (2019) 39–50. https://doi.org/10.1016/j.colsurfa.2018.12.028.

[3] M.F. López, J.A. Jiménez, A. Gutiérrez, XPS characterization of surface modified titanium alloys for use as biomaterials, Vacuum. 85 (2011) 1076–1079. https://doi.org/10.1016/j.vacuum.2011.03.006.

[4] R. Bayón, A. Igartua, J.J. González, U. Ruiz de Gopegui, Influence of the carbon content on the corrosion and tribocorrosion performance of Ti-DLC coatings for biomedical alloys, Tribol. Int. 88 (2015) 115–125. https://doi.org/10.1016/j.triboint.2015.03.007.

[5] J. Fojt, L. Joska, J. Málek, Corrosion behaviour of porous Ti–39Nb alloy for biomedical applications, Corros. Sci. 71 (2013) 78–83. https://doi.org/10.1016/j.corsci.2013.03.007.

[6] Y. Okazaki, E. Gotoh, Comparison of metal release from various metallic biomaterials in vitro, Biomaterials. 26 (2005) 11–21. https://doi.org/10.1016/j.biomaterials.2004.02.005.

[7] S.B. Gabriel, J.V.P. Panaino, I.D. Santos, L.S. Araujo, P.R. Mei, L.H. de Almeida, C.A. Nunes, Characterization of a new beta titanium alloy, Ti–12Mo–3Nb, for biomedical applications, J. Alloys Compd. 536 (2012) S208–S210. https://doi.org/10.1016/j.jallcom.2011.11.035.

[8] A. Ochsenbein, F. Chai, S. Winter, M. Traisnel, J. Breme, H.F. Hildebrand, Osteoblast responses to different oxide coatings produced by the sol–gel process on titanium substrates, Acta Biomater. 4 (2008) 1506–1517. https://doi.org/10.1016/j.actbio.2008.03.012.

[9] J.C. Lim, K.J. Song, C. Park, The effect of deposition parameters on the phase of TiO2 films grown by RF magnetron sputtering, J. Korean Phys. Soc. 65 (2014) 1896–1902. https://doi.org/10.3938/jkps.65.1896.

[10] O. Carp, C.L. Huisman, A. Reller, Photoinduced reactivity of titanium dioxide, Prog. Solid State Chem. 32 (2004) 33–177. https://doi.org/10.1016/j.progsolidstchem.2004.08.001.

[11] H.N. Pantaroto, A.P. Ricomini-Filho, M.M. Bertolini, J.H.D. Silva, N.F. Azevedo Neto, C. Sukotjo, E.C. Rangel, V.A.R. Barão, Antibacterial photocatalytic activity of different crystalline TiO2phases in oral multispecies biofilm, Dent. Mater. 34 (2018) e182–e195. https://doi.org/10.1016/j.dental.2018.03.011.

[12] K. Shahramian, A. Abdulmajeed, I. Kangasniemi, E. Söderling, T. Närhi, TiO 2 Coating and UV Photofunctionalization Enhance Blood Coagulation on Zirconia Surfaces, Biomed Res. Int. 2019 (2019) 1–9. https://doi.org/10.1155/2019/8078230.

[13] E. Westas, M. Hayashi, F. Cecchinato, A. Wennerberg, M. Andersson, R. Jimbo, J.R. Davies, Bactericidal effect of photocatalytically-active nanostructured TiO_2 surfaces on biofilms of the early oral colonizer, *Streptococcus oralis*, J. Biomed. Mater. Res. Part A. 105 (2017) 2321–2328. https://doi.org/10.1002/jbm.a.36086.

[14] E. Beltrán-Partida, B. Valdez-Salas, M. Curiel-Álvarez, S. Castillo-Uribe, A. Escamilla, N. Nedev, Enhanced antifungal activity by disinfected titanium dioxide nanotubes via reduced nano-adhesion bonds, Mater. Sci. Eng. C. 76 (2017) 59–65. https://doi.org/10.1016/j.msec.2017.02.153.

[15] P. Liu, Y. Hao, Y. Zhao, Z. Yuan, Y. Ding, K. Cai, Surface modification of titanium substrates for enhanced osteogenetic and antibacterial properties, Colloids Surfaces B Biointerfaces. 160 (2017) 110–116. https://doi.org/10.1016/j.colsurfb.2017.08.044.

[16] F. Rupp, M. Haupt, M. Eichler, C. Doering, H. Klostermann, L. Scheideler, S. Lachmann, C. Oehr, H.P. Wendel, E. Decker, J. Geis-Gerstorfer, C. von Ohle, Formation and Photocatalytic Decomposition of a Pellicle on Anatase Surfaces, J. Dent. Res. 91 (2012) 104–109. https://doi.org/10.1177/0022034511424901.

[17] S. Cao, B. Liu, L. Fan, Z. Yue, B. Liu, B. Cao, Highly antibacterial activity of N-doped TiO2 thin films coated on stainless steel brackets under visible light irradiation, Appl. Surf. Sci. 309 (2014) 119–127. https://doi.org/10.1016/j.apsusc.2014.04.198.

[18] J.-Y. Choi, C.J. Chung, K.-T. Oh, Y.-J. Choi, K.-H. Kim, Photocatalytic Antibacterial Effect of TiO 2 Film of TiAg on Streptococcus mutans, Angle Orthod. 79 (2009) 528–532. https://doi.org/10.2319/012108-169.1.

[19] H. Yaghoubi, N. Taghavinia, E.K. Alamdari, A.A. Volinsky, Nanomechanical Properties of TiO 2 Granular Thin Films, ACS Appl. Mater. Interfaces. 2 (2010) 2629–2636. https://doi.org/10.1021/am100455q.

[20] S. Mráz, J.M. Schneider, Structure evolution of magnetron sputtered TiO2 thin films, J. Appl. Phys. 109 (2011) 023512. https://doi.org/10.1063/1.3536635.

[21] F. Lebre, R. Sridharan, M.J. Sawkins, D.J. Kelly, F.J. O'Brien, E.C. Lavelle, The shape and size of hydroxyapatite particles dictate inflammatory responses following implantation, Sci. Rep. 7 (2017) 2922. https://doi.org/10.1038/s41598-017-03086-0.

[22] M.H. Ahmed, T.E. Keyes, J.A. Byrne, C.W. Blackledge, J.W. Hamilton, Adsorption and photocatalytic degradation of human serum albumin on TiO2 and Ag–TiO2 films, J. Photochem. Photobiol. A Chem. 222 (2011) 123–131. https://doi.org/10.1016/j.jphotochem.2011.05.011.

[23] A. Marucco, I. Fenoglio, F. Turci, B. Fubini, Interaction of fibrinogen and albumin with titanium dioxide nanoparticles of different crystalline phases, J. Phys. Conf. Ser. 429 (2013) 012014. https://doi.org/10.1088/1742-6596/429/1/012014.

[24] N. Huang, P. Yang, Y.X. Leng, J.Y. Chen, H. Sun, J. Wang, G.J. Wang, P.D. Ding, T.F. Xi, Y. Leng, Hemocompatibility of titanium oxide films, Biomaterials. 24 (2003) 2177–2187. https://doi.org/10.1016/S0142-9612(03)00046-2.

[25] V. Milleret, S. Buzzi, P. Gehrig, A. Ziogas, J. Grossmann, K. Schilcher, A.S. Zinkernagel, A. Zucker, M. Ehrbar, Protein adsorption steers blood contact activation on engineered cobalt chromium alloy oxide layers, Acta Biomater. 24 (2015) 343–351. https://doi.org/10.1016/j.actbio.2015.06.020.

[26] M. Roy, A. Pompella, J. Kubacki, J. Szade, R.A. Roy, W. Hedzelek, Photofunctionalization of Titanium: An Alternative Explanation of Its Chemical-Physical Mechanism, PLoS One. 11 (2016) e0157481. https://doi.org/10.1371/journal.pone.0157481.

[27] M. Li, L. Gao, J. Chen, Y. Zhang, J. Wang, X. Lu, K. Duan, J. Weng, B. Feng, Controllable release of interleukin-4 in double-layer sol–gel coatings on TiO 2 nanotubes for modulating macrophage polarization, Biomed. Mater. 13 (2018) 045008. https://doi.org/10.1088/1748-605X/aa9526.

[28] S. Gowtham, T. Arunnellaiappan, N. Rameshbabu, An investigation on pulsed DC plasma electrolytic oxidation of cp-Ti and its corrosion behaviour in simulated body fluid, Surf. Coatings Technol. 301 (2016) 63–73. https://doi.org/10.1016/j.surfcoat.2016.02.043.

[29] T. Kokubo, H. Takadama, How useful is SBF in predicting in vivo bone bioactivity?, Biomaterials. 27 (2006) 2907–2915. https://doi.org/10.1016/j.biomaterials.2006.01.017.

[30] V.A.R. Barão, M.T. Mathew, W.G. Assunção, J.C.-C. Yuan, M.A. Wimmer, C. Sukotjo, Stability of cp-Ti and Ti-6Al-4V alloy for dental implants as a function of saliva pH - an electrochemical study, Clin. Oral Implants Res. 23 (2012) 1055–1062. https://doi.org/10.1111/j.1600-0501.2011.02265.x.

[31] A.L.J. Pereira, P.N. Lisboa, J. Acuna, I.S. Brandt, A.A. Pasa, A.R. Zanatta, J. Vilcarromero, A. Beltran, J.H.D. da Silva, Enhancement of optical absorption by modulation of the oxygen flow of TiO2 films deposited by reactive sputtering, J. Appl. Phys. 111 (2012) 1–11. https://doi.org/10.1063/1.4724334.

[32] E. Combe, A protocol for determining the surface free energy of dental materials, Dent. Mater. 20 (2004) 262–268. https://doi.org/10.1016/S0109-5641(03)00102-7.

[33] J.M. Cordeiro, H.N. Pantaroto, E.M. Paschoaleto, E.C. Rangel, N.C. d. Cruz, C. Sukotjo, V.A.R. Barão, Synthesis of biofunctional coating for a TiZr alloy: Surface, electrochemical, and biological characterizations, Appl. Surf. Sci. 452 (2018) 268–278. https://doi.org/10.1016/j.apsusc.2018.05.044.

[34] T. Beline, I.D.S.V. Marques, A.O. Matos, E.S. Ogawa, A.P. Ricomini-Filho, E.C. Rangel, N.C. da Cruz, C. Sukotjo, M.T. Mathew, R. Landers, R.L.X. Consani, M.F. Mesquita, V.A.R. Barão, Production of a biofunctional titanium surface using plasma electrolytic oxidation and glow-discharge plasma for biomedical applications., Biointerphases. 11 (2016) 011013. https://doi.org/10.1116/1.4944061.

[35] R.R. Behera, A. Das, D. Pamu, L.M. Pandey, M.R. Sankar, Mechano-tribological properties and in vitro bioactivity of biphasic calcium phosphate coating on Ti-6Al-4V, J. Mech. Behav. Biomed. Mater. 86 (2018) 143–157. https://doi.org/10.1016/j.jmbbm.2018.06.020.

[36] J.M. Cordeiro, B.E. Nagay, A.L.R. Ribeiro, N.C. da Cruz, E.C. Rangel, L.M.G. Fais, L.G. Vaz, V.A.R. Barão, Functionalization of an experimental Ti-Nb-Zr-Ta alloy with a biomimetic coating produced by plasma electrolytic oxidation, J. Alloys Compd. 770 (2019) 1038–1048. https://doi.org/10.1016/j.jallcom.2018.08.154.

[37] H. Wang, R. Zhang, Z. Yuan, X. Shu, E. Liu, Z. Han, A comparative study of the corrosion performance of titanium (Ti), titanium nitride (TiN), titanium dioxide (TiO2) and nitrogen-doped titanium oxides (N–TiO2), as coatings for biomedical applications, Ceram. Int. 41 (2015) 11844–11851. https://doi.org/10.1016/j.ceramint.2015.05.153.

[38] B. Wang, S. Wei, L. Guo, Y. Wang, Y. Liang, B. Xu, F. Pan, A. Tang, X. Chen, Effect of deposition parameters on properties of TiO2 films deposited by reactive magnetron sputtering, Ceram. Int. 43 (2017) 10991–10998. https://doi.org/10.1016/j.ceramint.2017.05.139.

[39] U. Diebold, The surface science of titanium dioxide, Surf. Sci. Rep. 48 (2003) 53–229.

https://doi.org/10.1016/S0167-5729(02)00100-0.

[40] A. Kozlovskiy, I. Shlimas, K. Dukenbayev, M. Zdorovets, Structure and corrosion properties of thin TiO2 films obtained by magnetron sputtering, Vacuum. 164 (2019) 224–232. https://doi.org/10.1016/j.vacuum.2019.03.026.

[41] K. Shukla, R. Rane, J. Alphonsa, P. Maity, S. Mukherjee, Structural, mechanical and corrosion resistance properties of Ti/TiN bilayers deposited by magnetron sputtering on AISI 316L, Surf. Coatings Technol. 324 (2017) 167–174. https://doi.org/10.1016/j.surfcoat.2017.05.075.

[42] V. Barranco, M.L. Escudero, M.C. García-Alonso, 3D, chemical and electrochemical characterization of blasted TI6Al4V surfaces: Its influence on the corrosion behaviour, Electrochim. Acta. 52 (2007) 4374–4384. https://doi.org/10.1016/j.electacta.2006.12.031.

[43] J.M. Cordeiro, L.P. Faverani, C.R. Grandini, E.C. Rangel, N.C. da Cruz, F.H. Nociti Junior, A.B. Almeida, F.B. Vicente, B.R.G. Morais, V.A.R. Barão, W.G. Assunção, Characterization of chemically treated Ti-Zr system alloys for dental implant application, Mater. Sci. Eng. C. 92 (2018) 849–861. https://doi.org/10.1016/j.msec.2018.07.046.

[44] Q. Abbas, M. Mirzaeian, A.A. Ogwu, M. Mazur, D. Gibson, Effect of physical activation/surface functional groups on wettability and electrochemical performance of carbon/activated carbon aerogels based electrode materials for electrochemical capacitors, Int. J. Hydrogen Energy. (2018) 1–10. https://doi.org/10.1016/j.ijhydene.2018.04.099.

[45] D.A.H. Hanaor, C.C. Sorrell, Review of the anatase to rutile phase transformation, J. Mater. Sci. 46 (2011) 855–874. https://doi.org/10.1007/s10853-010-5113-0.

[46] P.I. Gouma, M.J. Mills, Anatase-to-Rutile Transformation in Titania Powders, J. Am. Ceram. Soc. 84 (2001) 619–622. https://doi.org/10.1111/j.1151-2916.2001.tb00709.x.

[47] V.C. Anitha, J.-H. Lee, J. Lee, A. Narayan Banerjee, S. Woo Joo, B. Ki Min, Biofilm formation on a TiO2 nanotube with controlled pore diameter and surface wettability., Nanotechnology. 26 (2015) 065102. https://doi.org/10.1088/0957-4484/26/6/065102.

[48] A. Giacomello, S. Meloni, M. Chinappi, C.M. Casciola, Cassie–Baxter and Wenzel States on a Nanostructured Surface: Phase Diagram, Metastabilities, and Transition Mechanism by Atomistic Free Energy Calculations, Langmuir. 28 (2012) 10764–10772. https://doi.org/10.1021/la3018453.

[49] R.A. Gittens, L. Scheideler, F. Rupp, S.L. Hyzy, J. Geis-Gerstorfer, Z. Schwartz, B.D. Boyan, A review on the wettability of dental implant surfaces II: Biological and clinical aspects, Acta Biomater. 10 (2014) 2907–2918. https://doi.org/10.1016/j.actbio.2014.03.032.

[50] M. Lorenzetti, G. Bernardini, T. Luxbacher, A. Santucci, S. Kobe, S. Novak, Surface properties of nanocrystalline TiO 2 coatings in relation to the in vitro plasma protein adsorption, Biomed. Mater. 10 (2015) 045012. https://doi.org/10.1088/1748-6041/10/4/045012.

[51] F.Y. Oliva, L.B. Avalle, O.R. Cámara, C.P. De Pauli, Adsorption of human serum albumin (HSA) onto colloidal TiO2 particles, Part I, J. Colloid Interface Sci. 261 (2003) 299–311. https://doi.org/10.1016/S0021-9797(03)00029-8.

[52] X. Liu, P. Chu, C. Ding, Surface modification of titanium, titanium alloys, and related materials for biomedical applications, Mater. Sci. Eng. R Reports. 47 (2004) 49–121.

https://doi.org/10.1016/j.mser.2004.11.001.

[53] M. Lilja, A. Genvad, M. Åstrand, M. Strømme, H. Enqvist, Influence of microstructure and chemical composition of sputter deposited TiO2 thin films on in vitro bioactivity, J. Mater. Sci. Mater. Med. 22 (2011) 2727–2734. https://doi.org/10.1007/s10856-011-4465-6.

[54] M.-G. Ma, Hierarchically nanostructured hydroxyapatite: hydrothermal synthesis, morphology control, growth mechanism, and biological activity, Int. J. Nanomedicine. 7 (2012) 1781. https://doi.org/10.2147/IJN.S29884.

2.2 Artigo: Outlining cell interaction and inflammatory cytokines on UV-photofunctionalized mixed-phase TiO_2 thin film

Heloisa Navarro Pantaroto[a], Amanda Bandeira de Almeida[a], Orisson Ponce Gomes[b], Adaias Oliveira Matos[a], Richard Landers[c], Renato Corrêa Viana Casarin[a], José Humberto Dias da Silva[b], Francisco Humberto Nociti Junior[a], Valentim Adelino R. Barão[a,*]

[a] *University of Campinas (UNICAMP), Piracicaba Dental School, Department of Prosthodontics and Periodontology, Av. Limeira, 901, Piracicaba, São Paulo, 13414-903, Brazil,*

[b] *São Paulo State University (UNESP), Department of Physics, Av. Eng. Luís Edmundo C. Coube, 14-01, Bauru, São Paulo 17033-360, Brazil*

[c] *University of Campinas (UNICAMP), Gleb Wataghin Physics Institute, Department of Applied Physics, R. Sérgio Buarque de Holanda, 777, Campinas, São Paulo, 13083-859, Brazil,*

Submitted on Applied Surface Science Journal.

Declarations of interest: none.

***** *Corresponding author.* Fax: +55-19-2106 5218.

E-mail address: vbarao@unicamp.br (V. Barão).

Abstract

UV photofunctionalization has been reported as an approach to improve physico-chemical and biological performance of titanium (Ti). This *in vitro* study determined the impact of UV-photofunctionalized mixed-phase TiO_2 films on physico-chemical properties of Ti discs and cell biology. Anatase-rutile TiO_2 films were grown by magnetron sputtering on commercially pure titanium (cpTi) discs, and samples were divided as follow: cpTi (negative control), TiO_2 (positive control), cpTi UV, TiO_2 UV (experimental). Surfaces were analyzed in terms of morphology, topography, chemical composition, crystalline phase and wettability. Pre-osteoblastic cells (MC3T3E1) were used to assess cell morphology and adhesion, viability, mineralization potential and cytokine expression (IFN-γ, TNF-α, IL-4, IL-6 and IL-17). TiO_2-coated surfaces exhibited granular surface morphology and greater roughness. Photofunctionalization increased wettability on both surface conditions ($p<.05$). TiO_2-treated groups featured normal cell morphology and spreading, and greater cellular metabolic activity at 2 and 4 days ($p<.05$), whereas UV-photofunctionalized surfaces enhanced cell metabolism and increased mineral nodule formation (day 14) ($p<.05$). In general, assessed proteins were found slightly affected by either UV or TiO_2 treatments. Altogether, the findings suggest that UV-photofunctionalized TiO_2 has the potential to improve the ability of cells to form mineral nodules by modifying Ti physico-chemical properties towards a more stable context.

Key words:

Titanium oxide; Sputtering; Titanium; Ultraviolet Therapy; Osteoblasts; Cytokines.

Highlights:

1. Mixed TiO_2 + UV-photofunctionalization enhanced cell metabolism and adhesion.
2. UV-photofunctionalization increased mineral nodule formation *in vitro*.
3. Some inflammatory markers were slightly affected by either UV or TiO_2 treatments.

Graphical abstract

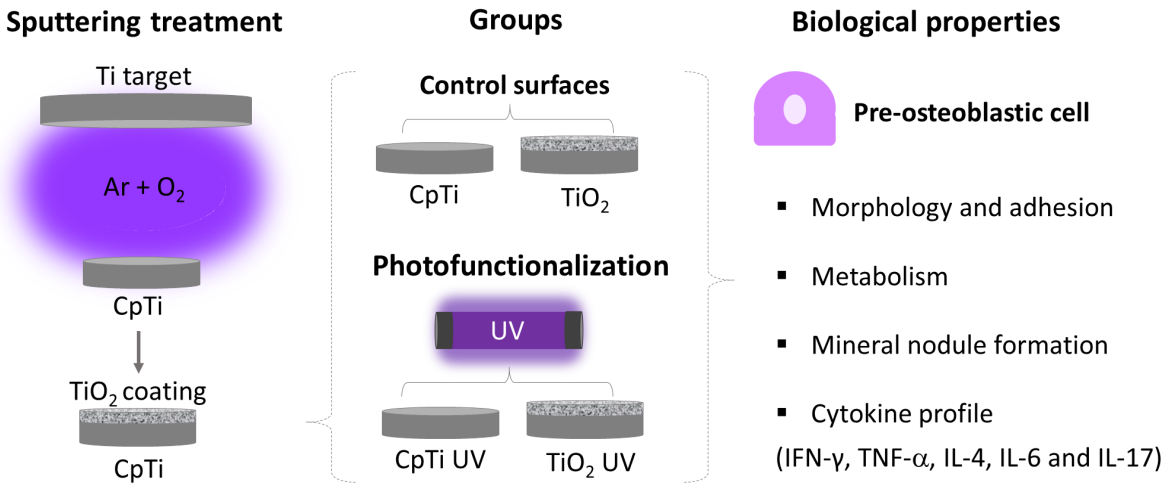

1. Introduction

High success rates have been reported for implant-supported dental prosthetic rehabilitation. Bone healing around dental implants is a coordinated and sequentially organized repair mechanism of the organism [1]. This process involves cytokine secretion, which coordinates the healing process along with proteins and cells. New bone formation begins with the secretion of a collagen matrix by osteoblasts [1], being crucial for inducing interfacial bone formation or osseointegration [2]. However, implant placement is not always possible on "ideal" conditions, and unfavorable conditions may eventually affect success rates and long-term outcomes. Thus, it is of utmost importance to develop methods that could enhance and/or improve wound healing around titanium (Ti) implants [3] in order to enhance treatment predictability. Currently Ti is the preferred material to produce dental implants with the potential to achieve osseointegration [4]; however after manufacturing, Ti is susceptible to a natural surface aging, which may account for a loss of bioactivity [5,6]. As an attempt to produce more stable metal surfaces, photofunctionalization has been proposed as a viable method [5,6].

Photofunctionalization is an ultraviolet light (UV) pretreatment on the implant surface previously to its implantation. Importantly, photofunctionalized surfaces are known to be osteoconductive [6]. In addition, *in vitro* and *in vivo* studies have shown that photofunctionalization of machined Ti and Ti-treated surface is effective, and may provide a complete and faster bone-implant interface [3,6–13]. While photofunctionalization has been

reported to affect chemical and wettability properties of Ti surfaces [5,6], the presence of titanium dioxide (TiO_2) has been suggested as an enhancer for such an effect [6]. A recent study have investigated the effect of UV-photofunctionalization on crystalline mixed-phase TiO_2 obtained by alkali and heat treatment, and demonstrated that UV irradiation was able to improve biocompatibility and antimicrobial properties of TiO_2 [3]. Although, some progress has been made to understand the potential of photofunctionalization to improve surface properties of Ti-made materials, there is a lack of evidence to establish the most effective approach. Magnetron sputtering is a suitable and simple method to deposit crystalline TiO_2 films with the advantages of resulting in greater film adhesion, hardness, hydrophilicity and low cost [14–17]. The potential of UV-photofunctionalization on magnetron-sputtered TiO_2 films remains unknown. In the current investigation, we hypothesized that UV-photofunctionalization on magnetron-sputtered TiO_2 films created on Ti discs would significantly improve their physico-chemical and biological properties.

2. Materials and methods

2.1 Experimental design

Commercially pure titanium (cpTi) discs (grade 2 as per the ASTM) (15 mm diameter × 1 mm thickness) (Realum, Vila Prudente, São Paulo, Brazil) were used. TiO_2-coated cpTi samples were submitted to radiofrequency (RF) magnetron sputtering technique to obtain crystalline TiO_2 films composed of anatase and rutile. Afterwards, cpTi and TiO_2-coated cpTi samples were submitted to UV photofunctionalization. Thus, the studied groups were: 1. cpTi (negative control); 2. cpTi UV; 3. TiO_2 and 4. TiO_2 UV. Samples' surfaces were characterized based on their chemical composition, crystalline phase, morphology and wettability (contact angle measurement). *In vitro* cell behavior was evaluated considering the morphology, viability, mineralization potential and cytokine expression of a pre-osteoblastic cell line (MC3T3-E1). The experimental design is summarized on Fig. 1.

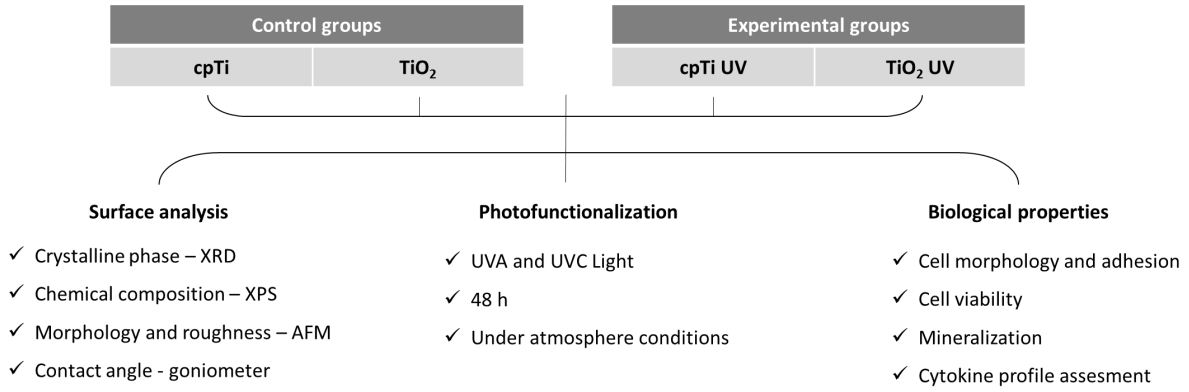

Figure 1. Experimental design.

2.2 Sample preparation

In order to obtain a homogeneous TiO_2 film deposition, discs were polished using sequential SiC grinding papers (#320, #400 and #600) (Carbimet 2, Buehler, Lake Bluff, IL, USA) in an automatic polisher (EcoMet/AutoMet 250 Pro, Buehler). Next, discs were mirror finished with diamond paste (MetaDi 9- micron, Buehler), lubricant (MetaDi Fluid, Buehler) and polishing cloth (TextMet Polishing Cloth, Buehler). Finally, a colloidal silica polishing suspension (MasterMed, Buehler) was used with a ChemoMet I polishing cloth (Buehler). Samples were ultrasonically cleaned in deionized water (10 min) and degreased in 70% propanol (10 min) (Sigma-Aldrich, St. Louis, MO, USA) and hot air dried [18].

2.2.1 Mixed-phase crystalline TiO_2 film deposition

TiO_2 films were grown by a radiofrequency magnetron sputtering in a Kurt J. Lesker sputtering chamber (model KJL—System I). A Ti-metal target (99.999%) (AJA International, North Scituate, MA, USA) was used in a Torus 3" sputtering gun. Before each deposition, the target was sputtered with Ar for 10 min to ensure that its surface is clean during the growth of the films [19]. The parameters used, developed in a previous investigation [20] are shown in Table 1. Sputtered samples were individually stored on dust free small bags before the surface analysis, and for the biological tests samples were previously sterilized by gamma radiation (14.50 ± 0.05 kGy) [21].

Table 1. Deposition parameters of TiO_2 films grown by RF magnetron sputtering.

Ar flux	O_2 flux	Pressure	RF Power	Total time deposition	Heater temperature
40 SCCM	1 SCCM	1.2×10^{-2} Torr	240 W	12 h	400 °C

2.2.2 UV-photofunctionalization procedure

Photofunctionalization was performed in the cpTi UV and TiO_2 UV samples in a customized light apparatus coupled with UVA (360 nm - 40 W) and UVC lamps (250 nm - 40 W) for 48 h [5,10]. Photofunctionalized surfaces were used immediately (fresh surface) for surface analysis and cell culture.

2.3 Surface characterizations

Samples were submitted to surface characterization to confirm the TiO_2 incorporation, the presence of anatase and rutile crystalline phases. Furthermore, the wettability and morphology were also evaluated, considering that such properties are important for cell interaction [6,22–24].

2.3.1 Chemical composition and crystalline phase analysis

Chemical composition of the outmost oxide layer was determined by X-ray photoelectron spectroscopy (XPS) analysis (K-Alpha X-ray XPS, Thermo Scientific, Vantaa, Finland) employing an Al K Alpha source, energy step size of 0.1 eV and a spot size of 400 μm (n = 1). To investigate the crystalline phase, samples were analyzed by X-ray diffraction (XRD) (Rigaku-Ultima 2000+, Rigaku Corporation, Salem, NH, USA) using a Cu-K - λ = 1.54056 Å in operating radiation at 40 kV and 20 mA under continuous speed (0.02°/second) in a fixed angle (2.5°**)** and a scan range from 15° to 80° (n=1). Considering that photofunctionalization is not able to alter the crystalline phase [3] only cpTi and TiO_2 groups without UV light application were assessed.

2.3.2 Topography and morphology analyses

Surface topography was analyzed by atomic force microscopy (AFM) (Park System-NX-10; Park systems, Suwon, Korea), using a frequency of 320 kHz in a tapping mode with a constant force of 42 N/m. Two- and three-dimensional micrographs of 20×20 μm, 5×5 μm

and 1×1 μm were obtained. Roughness values arithmetic average (Ra) and root means square average (RMS) were obtained in three different areas of the 20×20 μm micrograph and the total surface area was estimated using a specific software (Gwyddion v 2.37; GNU General Public License; Czech Republic). Considering that photofunctionalization is not able to alter roughness [3,7,10] and topography [5,25], only cpTi and TiO_2 groups without UV light application were assessed (n=1).

2.3.3 Wettability

Contact angle was determined for all the studied surfaces using a goniometer (Ramé-Hart 100-00; Ramé-Hart Instrument Co., Succasunna, NJ, USA) by the sessile drop (15 mL) method through the Owens–Wendt approach (n=5). Briefly, two liquids with different polarities were used, water (polar component) and diiodomethane (dispersive component), and the contact angle measurements were performed using the Ramé-Hart DROP software (Ramé-Hart 100-00; Ramé-Hart Instrument Co., Succasunna, NJ, USA) [26]. Photofunctionalized surfaces were evaluated immediately and after 1, 2, 3, 4, 5 and 6 h after UV exposure.

2.4 Cell culture

In order to determine the impact of experimental and control surfaces on cell response, a pre-osteoblastic cell line (MC3T3-E1) was used. Cells were cultured in Minimum essential medium eagle – Alpha Modification (Alpha MEM: Gibco, Life Technologies, Gaithersburg, MD, USA) supplemented with 10% fetal bovine serum (FBS; Gibco, Life Technologies, Gaithersburg, MD, USA), penicillin (100 U/mL) in a humidified incubator at 37 °C and 5% CO_2 atmosphere. After reaching confluence (70%–80%), cells were detached using trypsinethylenediaminetetraacetic acid (Gibco, Life Technologies, Gaithersburg, MD, USA), centrifuged, and resuspended in culture medium for seeding over the previously gamma sterilized samples.

2.4.1 Cell morphology and adhesion

Cells were seeded on the samples in duplicate at 1.5×10^4 cells/mL in a 24-well plate in Alpha MEM supplemented with 10% FBS and antibiotics. After 24 h, the medium was replaced for Alpha MEM supplemented with 2% FBS plus antibiotics (day 0), which was

refreshed every other day. After 1, 2 and 4 days the culture medium was removed, cells were fixed using Karnovsky's solution (pH 7.4) overnight at 4°C and post-fixed in osmium tetraoxide (1%) for 1 h at room temperature. Samples were dehydrated in a series of increasing concentrations of ethanol washes (60%, 70%, 80%, 90% and 100%) for 10 min at room temperature, critical-point dried using CO_2 (Denton Vacuum, mod. DCP-1, Moorestown, NJ, USA) and gold sputtered (Bal-Tec, mod. SCD 050, Fürstentum, Liechtenstein) [27]. Cell morphology and adhesion were determined by scanning electron microscopy (SEM) (JEOL JSM-5600LV, Peabody, MA, USA) using 100×, 250× and 500× magnification. Experiments were performed at least twice with similar results.

2.4.2 Cellular metabolism assay

Cells were seeded (3×10^4 cells/mL) over the samples in a 24-well plate. At the end of the experimental periods, culture medium was removed and 900 µL of Alpha MEM with 100 µL of MTT (5 mg/mL) (Life Technologies, USA) was added and incubated at 37 °C and 5% CO_2 for 4 h. Subsequently, 500 µL of dimethyl sulfoxide (Sigma-Aldrich, USA) was added to each well to dissolve the formazan crystals produced by the cleavage of MTT salt in the mitochondria of viable cells. Cellular metabolic activity was determined at days 1, 2 and 4 days. Three aliquots (100 µL) of each sample were transferred to a 96-well plate and the optical density of the solution was read at 570 nm wavelength using an Elisa Reader (VersaMax, Molecular Devices, Sunnyvale, CA, USA). The obtained mean of the three readings of each sample was considered as a single value [28]. Experiments were performed in triplicate and at least twice with similar results.

2.4.3 In vitro mineral nodule formation assay

In order to determine the impact of control and experimental surfaces on cell differentiation and in vitro mineral nodule formation, cells were incubated in αMEM (Gibco, Life Technologies) with and without ascorbic acid, supplemented with 10% FBS (Gibco, Life Technologies) and antibiotic (penicillin/streptomycin) (10 µg/mL) (Gibco, Life Technologies) at 37 °C in a humidified atmosphere of 5% CO_2 for 4, 7 and 14 days. After each experimental period, cells were washed in PBS, fixed with 70% ethanol for 1 h and then, washed in NanoPure solution to remove the ethanol. Next, cells were stained with red Alizarin solution

(AR-S) at 37 °C for 10 min as previously reported [29] and aliquots (100 µL) of the solution from each sample were transferred to 96-well plate in triplicate to perform the absorbance reading in a spectrophotometer (562 nm) [29]. Experiments were performed in triplicate and, at least twice, with similar results.

2.4.4 Cytokine profile assessment

In order to define the impact of control and experimental surfaces on the expression of selected inflammatory markers, cells were seeded in triplicates (3×10^4 cells/well) in a 24-well plate and cultured for 1, 2 and 4 days. The secreted levels of interleukin (IL)-4, IL-6, IL-17, tumor necrosis factor (TNF)-α, and interferon (IFN)-γ were determined in the culture medium using the multiplexing technology following as previously reported [30]. Protein concentrations were estimated using a standard curve and a specific software (Xponent®Millipore Corporation, Billerica, MA, USA). The mean concentration of each biomarker was calculated and expressed as picogram per milliliter.

2.5 Statistical analysis

Two-way ANOVA analysis was used to evaluate the influence of surface treatment and time on the contact angle and cell metabolic activity (MTT). Mineral nodule formation was statistically analyzed by three-way ANOVA to investigate the effects of surface treatment, period and medium conditions. Tukey Honestly Significant Difference (HSD) test was used for post-hoc comparisons. Levels of cytokines were assessed using the non-parametric Kruskal-Wallis test to investigate the influence of surface treatment. Non-parametric Mann-Whitney U test was used to compare groups in pairs. For all the statistical analysis a p value of 0.05 was defined (IBM SPSS Statistics for Windows, v. 21.0., IBM Corp., Armonk, NY, USA).

3. Results

3.1 Physico-chemical characterizations of titanium surfaces

Chemical analysis of the outer layer formed on the surfaces of bare and TiO_2 coated cpTi substrates revealed the presence of Ti2p, oxygen (O1s) and carbon (C1s). The detailed spectra of the peaks and the atomic percentage of each compound are presented in Fig. 2.

Peaks of Ti such as Ti 2p1/2 and Ti 2p3/2 were detected and located at 463.6 eV and 458 eV, respectively [31–33]. There was a 5.6 eV energy difference between these peaks, which suggested that the oxidation state is Ti^{4+} in TiO_2 sites, as expected [34]. The oxygen peak positioned at 529 eV was associated to the bonding in the TiO_2 lattice, while the peak at 532 eV was related to O–H hydroxyl species and the peak correlated to C–O, which may represent contaminants most likely originating from the substrate polishing process [31–33]. The localization of surface peaks found suggests TiO_2 binding. Carbon contamination on Ti surfaces is typical and unavoidable due to its spontaneously adsorbing from ambient air onto the surface [33]. Two carbon peaks were observed, one at 284 eV representing a hydrocarbon species or impurities C–H/C–C and another peak located at 286 eV associated to C–O species [33] (Fig. 2a). In summary, photofunctionalization drastically reduced the C content and to increased Ti and O contents for both, atomic percentage and peak intensity. This event was even more evident for TiO_2 UV surfaces (Fig. 2b).

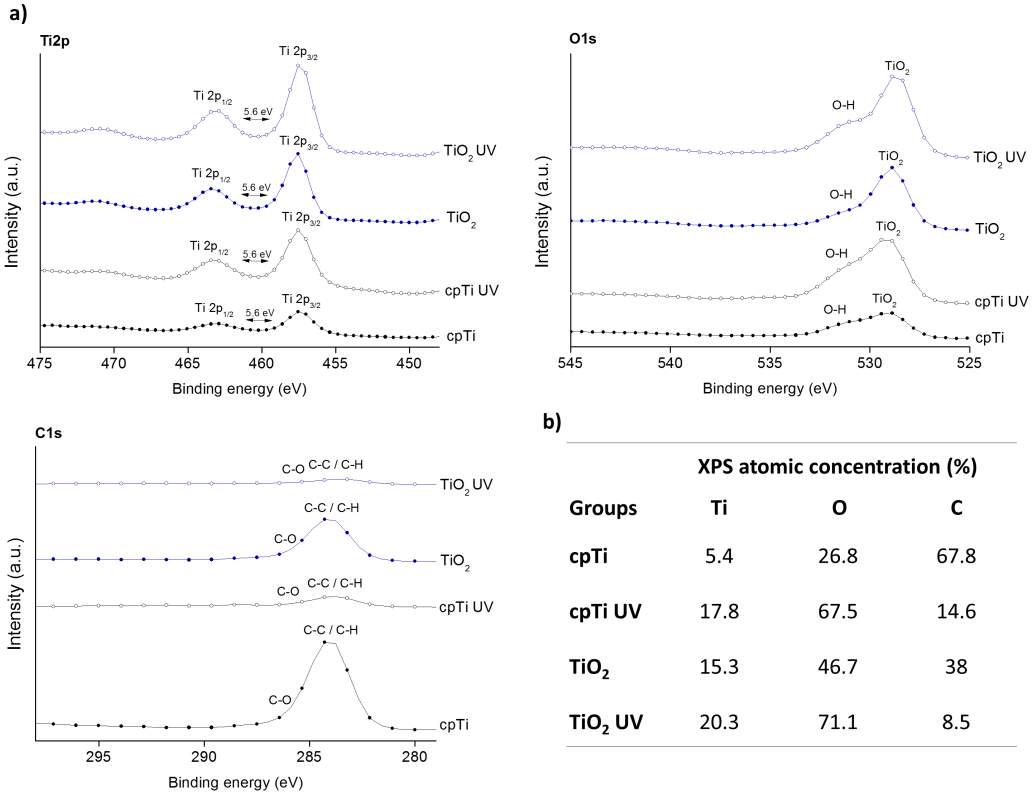

b)

	XPS atomic concentration (%)		
Groups	**Ti**	**O**	**C**
cpTi	5.4	26.8	67.8
cpTi UV	17.8	67.5	14.6
TiO_2	15.3	46.7	38
TiO_2 UV	20.3	71.1	8.5

Figure 2. (a) Detailed XPS spectra and (b) chemical composition (at%) for cpTi and TiO_2-coated surfaces before and after UV-photofunctionalization.

The crystalline phases of the samples were evaluated using an XRD (Fig. 3). The peaks found were Ti (T), Anatase (A) and Rutile (R) related to titanium and its oxide phases. Titanium peaks were found in all surfaces due to the substrate being made of titanium, whereas TiO_2 anatase and rutile peaks were found only for TiO_2 coated surfaces. Therefore, data analysis confirmed the successful incorporation of mixed-phase crystalline TiO_2 on the cpTi surfaces.

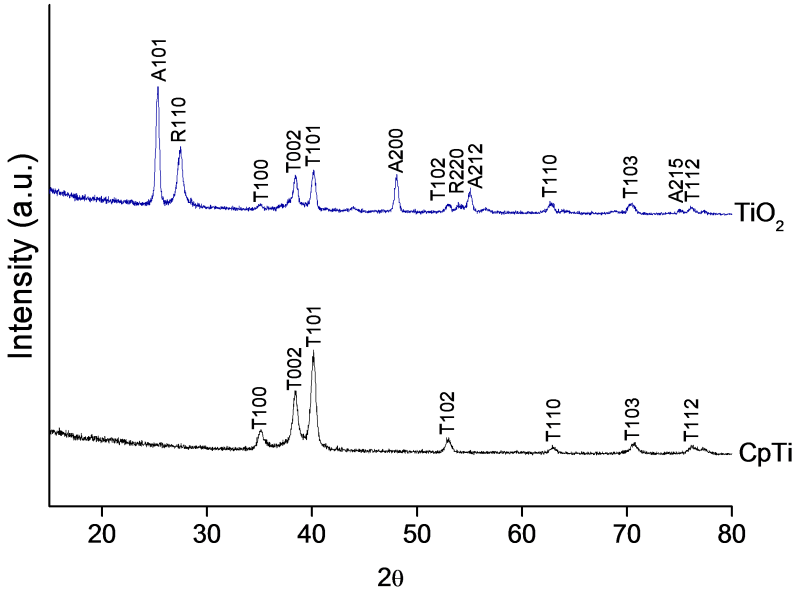

Figure 3. XRD pattern of surfaces for cpTi and TiO_2-coated surfaces (n = 1). Letters T, A and R refers to the corresponding peaks of titanium, anatase and rutile, respectively. The XRD spectra are reprinted (with modifications) from Dental Materials, Pantaroto et al. Antibacterial photocatalytic activity of different crystalline TiO_2 phases in oral multispecies biofilm, 34:182e195, 2018; Copyright (2020), with permission from Elsevier.

Fig. 4a shows the affinity of each surface with polar (water) and dispersive (diiodomethane) components by immediately measuring the contact angle of liquids. A contact angle below 90° suggests a great droplet spread and consequently a hydrophilic surface, whereas a contact angle above 90° means that the surface tends to hydrophobicity [35]. The smaller the contact angle, the greater the surface wettability. Despite all surfaces presenting a hydrophilic status, UV-photofunctionalization significantly reduced contact angle ($p<.05$). The water contact angle mean values of cpTi and TiO_2 was 84° and 90°, respectively, and 39° and 23° for cpTi UV and TiO_2 UV. In contrast, the diiodomethane contact angle was only slightly reduced by photofunctionalization. Furthermore, photofunctionalized surfaces displayed higher affinity with the polar component, which

means that the water sessile drop presented a greater spread on the surface. Nevertheless, the effect of photofunctionalization on the water contact angle presented a short life, where after 1 h of UV treatment the hydrophilic nature of both surfaces was attenuated (Fig. 4b).

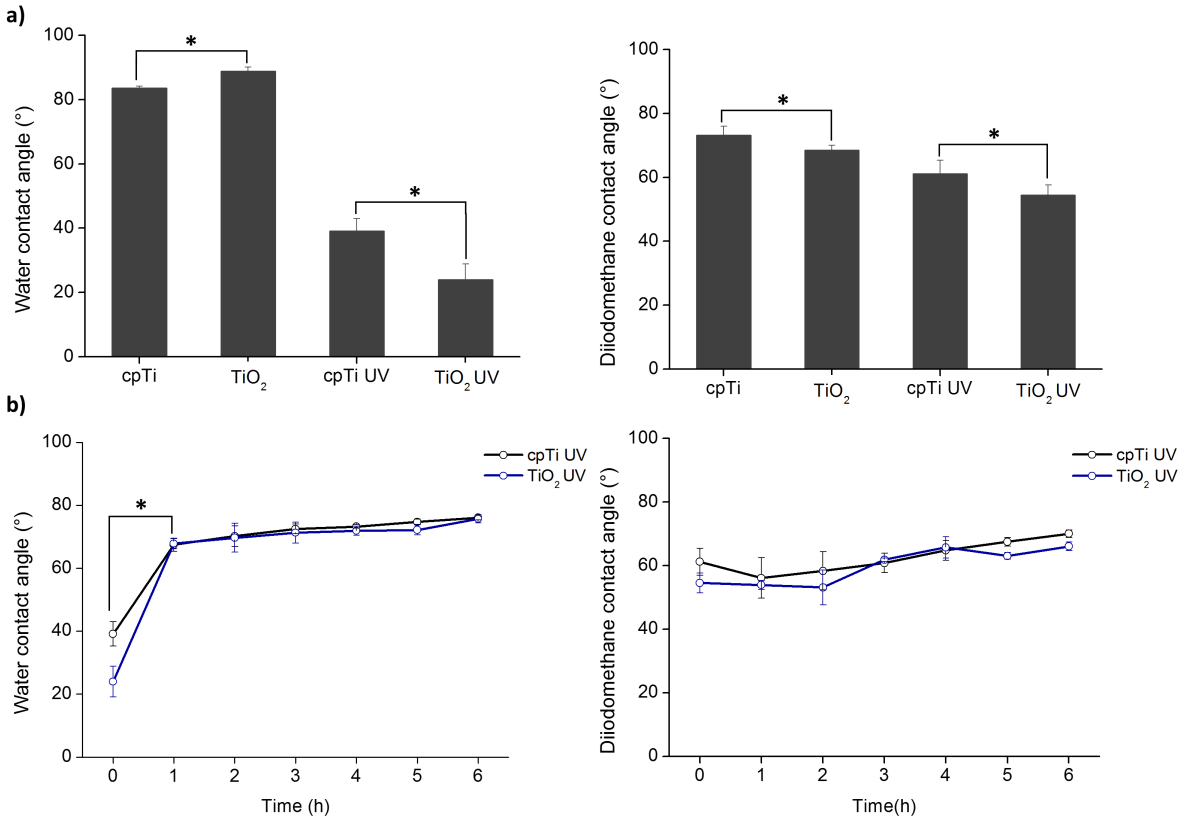

Figure 4. a) Immediate (0 h) water and diiodomethane contact angles for cpTi and TiO_2-coated surfaces before and after UV-photofunctionalization. b) hydrophilic status degradation (up to 6 h after UV treatment) for UV-photofunctionalized cpTi and TiO_2-coated surfaces. *$p<0.05$, using Tukey's HSD test.

Fig. 5 illustrates the morphology and topography of cpTi and TiO_2 surfaces. CpTi featured a smoother surface due to the mirror finishing procedure, whereas the TiO_2 surface showed a granular nature, suggesting TiO_2 nanoparticles incorporation. It is possible to note the presence of granules in different sizes, as a result of anatase (smaller granules) and rutile (larger granules) structures [36]. Additionally, TiO_2 film homogenously covered the substrate surface. A tridimensional profiling illustrates the peaks and valleys obtained of each surface. TiO_2 presented higher values of Ra and RMS in comparison to cpTi.

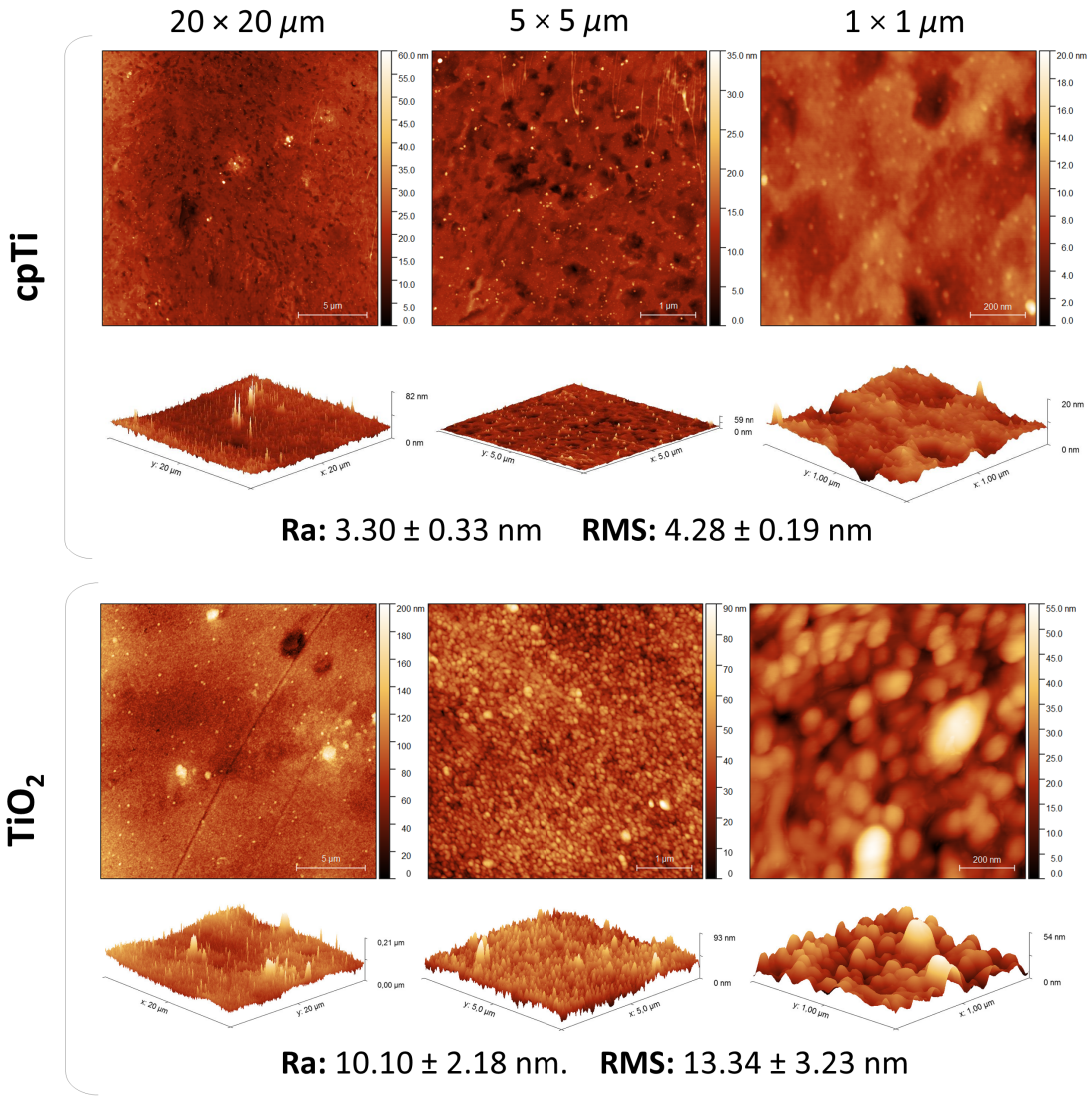

Figure 5. Topography, morphology, roughness average (Ra), root means square (RMS) for cpTi and TiO_2-coated surfaces before UV-photofunctionalization obtained by AFM.

3.2 Biological data

3.2.1 Cell morphology and adhesion

In order to evaluate cell adhesion, spreading and colonization on control and experimental Ti surfaces, SEM analysis was performed after 1, 2 and 4 days (Fig. 6). Overall, data analysis showed that cells cultured on TiO_2 and TiO_2 UV surfaces presented more cellular filopodia with a higher degree of extension, indicating a more favorable environment for cell migration [37]. These findings suggest that TiO_2 and UV-photofunctionalization are potential strategies to improve cell attachment.

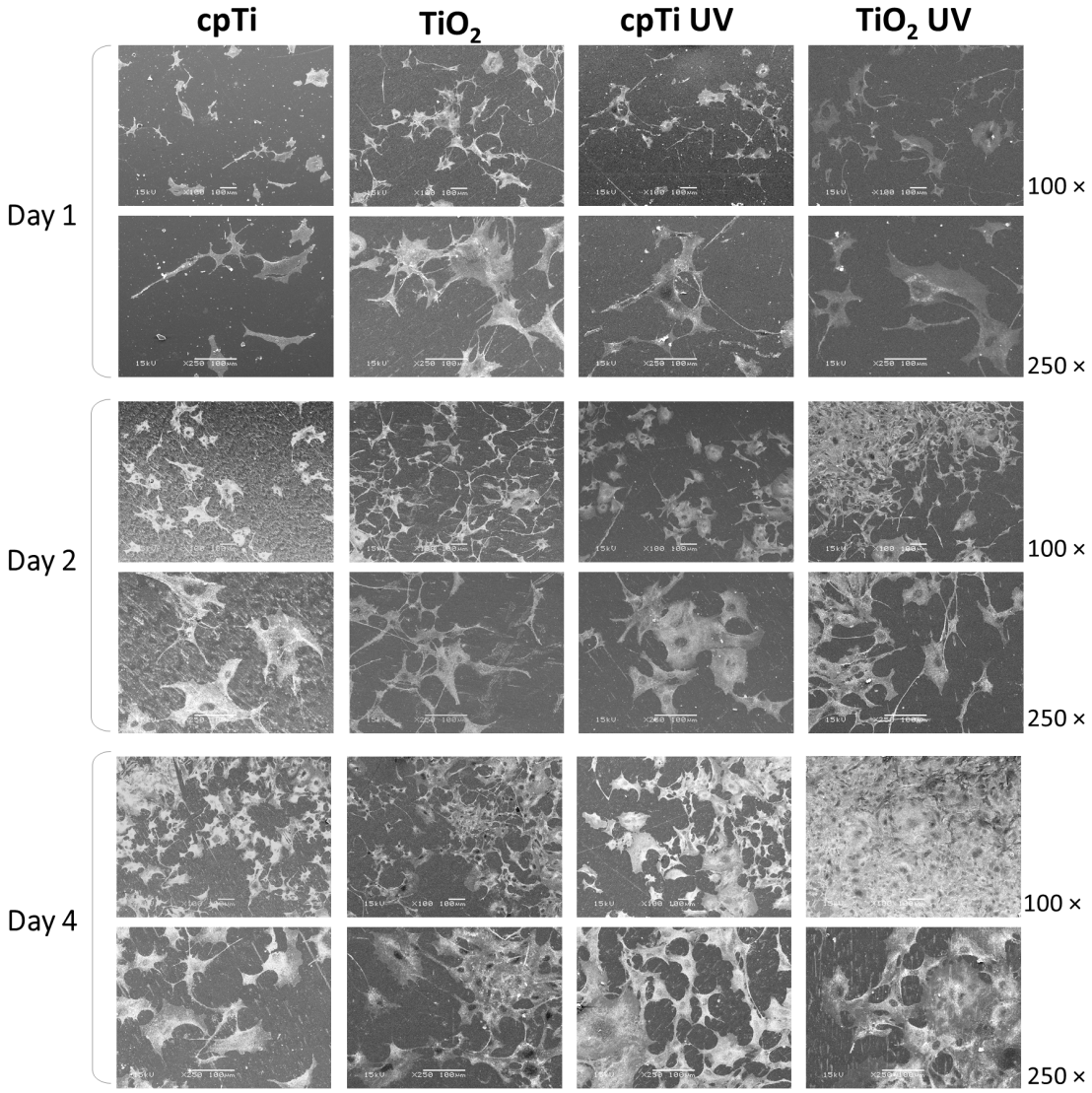

Figure 6. SEM micrographs of pre-osteoblastic MC3T3-E1 cells morphology and adhesion for cpTi and TiO_2-coated surfaces before and after UV-photofunctionalization after 1, 2 and 4 days of cell culture at 100× and 250× magnification using 15 kV.

3.2.2 Cell metabolism

In the current study, the impact of control and experimental surfaces in cell metabolism was assessed by the MTT assay at days 1, 2 and 4 (Fig. 7a). In general, intra-group analysis demonstrated that all the experimental groups displayed a significant increased metabolic activity at day 2 as compared to day 1 ($p<.05$), with a tendency of returning to the initial levels at day 4. Furthermore, inter-group analysis demonstrated that at day 2, TiO_2 UV featured the highest metabolic activity as compared to the other groups ($p<.05$) followed by

TiO_2, cpTi UV and cpTi. At day 4, inter-group analysis showed that the TiO_2 UV group continued to present higher metabolic activity as compared to the other groups ($p<.05$), but now followed by cpTi UV, TiO_2, and cpTi.

3.2.3 In vitro mineral nodule formation

In the current investigation, the potential of control and experimental surfaces to affect cell differentiation and mineral nodule formation was assessed by the alizarin red assay. Cells were cultured or not under differentiation conditions and statistically compared. Intra-group analysis revealed that the osteogenic condition distinctly affected the cells across the experimental groups, but in general resulted in a greater amount of mineralization starting as early as at 4 days for the TiO_2 group ($p<.05$). Importantly, inter-group analysis showed that UV-photofunctionalization, for both cpTi and TiO_2 groups, significantly affected the ability of MC3T3-E1 cells to produce mineral nodules under osteogenic conditions at day 14 ($p<.05$).

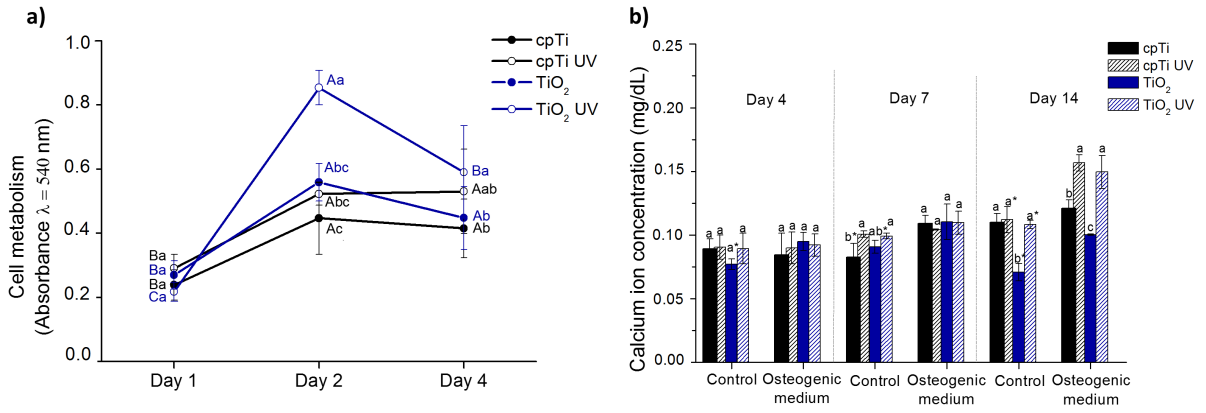

Figure 7. a) Viability of pre-osteoblastic MC3T3-E1 cells cultured for 1, 2 and 4 days on cpTi and TiO_2-coated surfaces before and after UV-photofunctionalization. Capital letters denote statistical differences between periods within each surface condition, while lower case letters represent statistical differences between groups within each period ($p<0.05$, Tukey's HSD test). b) Calcium ion concentration of pre-osteoblastic MC3T3-E1 cells cultured in non-osteogenic medium (control) and osteogenic medium for 4, 7 and 14 days on cpTi and TiO_2-coated surfaces before and after UV-photofunctionalization. Different letters indicate statistically significant differences between surfaces within each period and culture medium,

while asterisk represent statistical differences between culture medium within each surface and period ($p<0.05$, Tukey's HSD test).

3.2.4 *Secretome analysis*

In the current work, we determined whether or not control and experimental surfaces affected the expression of selected inflammatory markers at days 1, 2 and 4 (Fig. 8). In general, assessed proteins were found slightly affected by either UV or TiO_2 treatments and time. Inter-group analysis showed that the association of TiO_2 and UV photofunctionalization reduced the levels of IFN- γ at day 4, while it resulted in increased levels of IL-6 at the same time point ($p<0.05$). Data analysis further demonstrated that TNF-α, IL-4 and IL-17 secretion were not significantly affected by the experimental surfaces. Furthermore, intra-group analysis showed that at day 2, TNF-α secretion was increased in the cpTi UV and TiO_2 UV compared to day 1 ($p<0.05$), returning to the basal levels at day 4. In addition, IL-6 levels were decreased at day 2 as compared to day 1, and significantly increased at day 4 for the TiO_2 group ($p<0.05$).

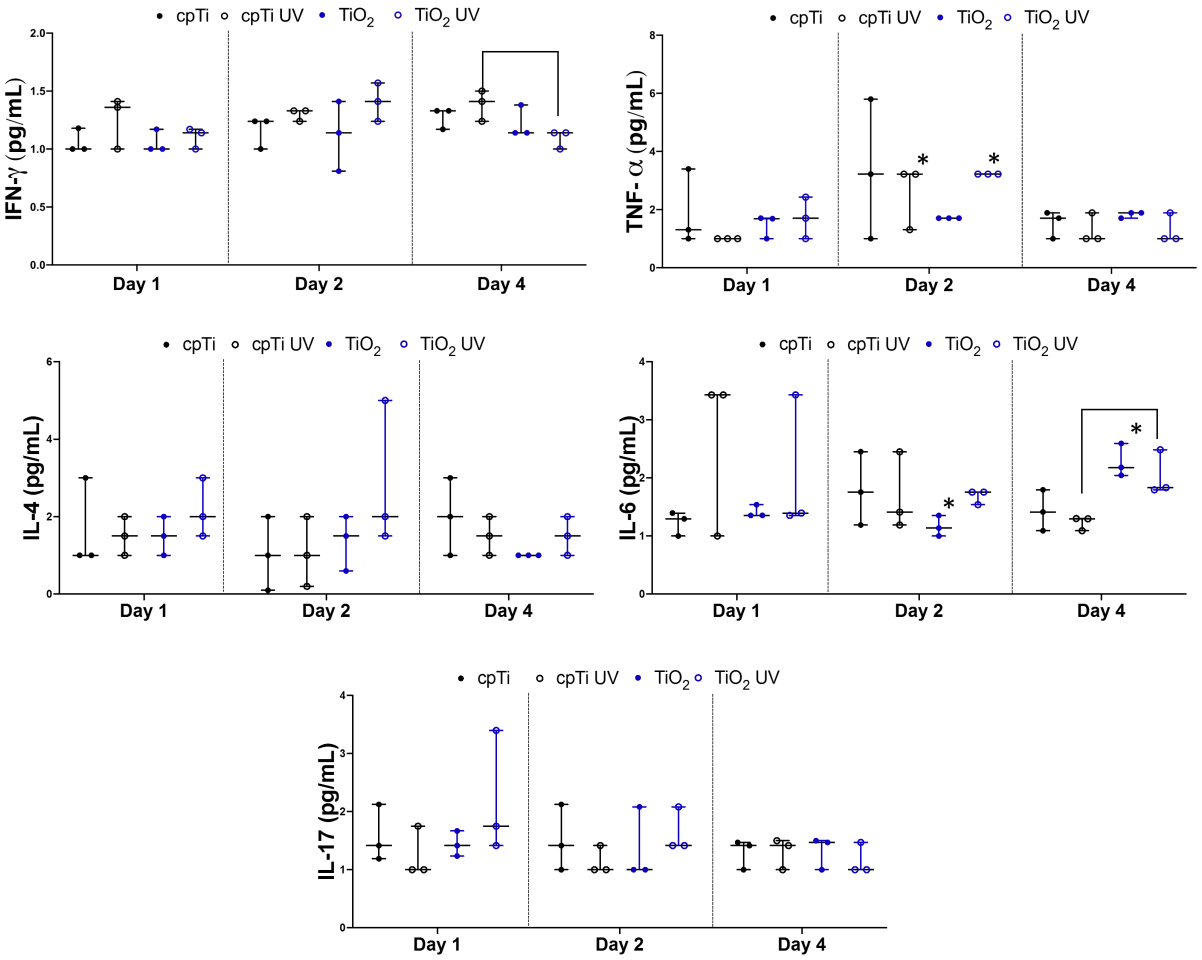

Figure 8. The expression of selected cytokines, including IFN-γ, TFNα, IL- 4, IL-6 and IL- 17, was determined in pre-osteoblastic MC3T3-E1 cells cultured in cpTi and TiO_2-coated surfaces before and after UV-photofunctionalization at days 1, 2 and 4. Bars indicate statistical inter-group differences within each period, whereas * indicates intra-group differences overtime compared with Day 1 ($p<0.05$, Mann-Whitney U test).

4. **Discussion**

This study investigated whether photofunctionalization of a mixed-phase crystalline TiO_2 film on cpTi surface would affect its physico-chemical and biological properties. Here, it was found that bi-phasic polycrystalline TiO_2 thin films were successfully grown by magnetron sputtering, obtaining a mix of anatase and rutile phases. Furthermore, in the present study, TiO_2 surface roughness (10 nm) was found to be close to the optimal roughness (Ra) value (13 and 16 nm) as previously proposed for cell culture interaction with a biomaterial [38]. It is now known that a more stable and strong surface resulting from the

presence of a crystalline structure [3,20], along with topography, wettability and chemical characteristics will play a key role on cell response [6,22–24]. The overall findings of the current investigation clearly demonstrate the potential of UV-photofunctionalized TiO_2 films created by magnetron sputtering treatment to modify Ti disc surface and modulate MC3T3-E1 cell physiologic characteristics towards an increased cell metabolism and higher ability to differentiate and produce mineral nodules *in vitro*.

In the present study, photofunctionalization significantly affected wettability of both, cpTi and TiO_2 surfaces. The photofunctionalized cpTi and TiO_2 surfaces presented a contact angle reduction of 53.5% and 73%, respectively, leading to a better wettability. This reduction in contact angle occurs due to the decreased percentage of atomic carbon [6] observed on photofunctionalized surfaces. Carbon is a common surface contaminant in Ti and Ti compounds [31] and after photofunctionalization, both C peaks and atomic% presented a great reduction on cpTi UV and TiO_2 UV surfaces. Additionally, TiO_2 UV presented a greater C reduction probably due to the TiO_2 photocatalytic action that promote great removal of hydrocarbons [6] compared to cpTi UV. In addition, cpTi has a thin Ti oxide layer naturally formed onto the surface [39,40], which is less stable than sputtered TiO_2. Intriguingly, such effect was not maintained overtime, where after 1 h of dry storage the increased hydrophilic nature of cpTi and TiO_2 surfaces was attenuated. A wet storage method using distilled H_2O has been suggested to maintain the achieved outcome of photofunctionalized surfaces for up to 28 days [41].

Exposure time and type of light are important factors in C removal from the surface. Despite some progress, there is a lack of evidence to define the most appropriate light apparatus and its usage time to produce optimal photofunctionalized metal surfaces. Existing data suggest that longer UV irradiation time may result in a greater effect by photofunctionalization [5,6,10]. Both UVA and UVC irradiation are able to modify the chemical properties of Ti surfaces without sacrificing its excellent physical characteristics; however UVC appears to be more effective for C removal, promoting a higher content of Ti–OH on the surface [25,42]. In the present study, UVA and UVC lights were used in order to obtain a higher spectrum of the light. The amount of C adsorbed on TiO_2 at the time of implant placement has been suggested as a critical factor to determine the initial affinity level for osteoblasts [6]. Here, C removal by photofunctionalization of both cpTi and TiO_2

surfaces may have indeed played an important role to modulate cell response, as pre-osteoblastic cells were found to have increased metabolic rates and a higher potential to produce mineral nodules when cultured on UV-photofunctionalized Ti discs. Altogether, the findings of the present work showed that the levels of C removal achieved by the methods used suggest that UV-photofunctionalization may induce cell differentiation *in vitro* leading to an enhanced process of biomineralization. Previous *in vitro* studies have indeed demonstrated that cell attachment, spreading, proliferation, alkaline phosphatase activity, and mineralization are enhanced by photofunctionalized surfaces structured with amorphous TiO_2 [6,8,10,11] and crystalline TiO_2 [3,7,12] compared to non-photofunctionalized surfaces. Additionally, enhanced platelet activation has been reported on photofunctionalized crystalline TiO_2 surface [13]. A potential rationale for the improved biological properties reported for photofunctionalized surfaces resides on the exposition of Ti^{4+} sites after C removal, promoting a positive charging onto the surface, which favours the interaction of negatively charged cells, such as osteoblasts [6]. Despite the fact that UV-photofunctionalization rises as a promising strategy to modulate host response, the present study is limited to an *in vitro* setup and additional *in vivo* studies should be proposed in order to prove this model as a valuable approach.

As an attempt to expand our knowledge on the potential mechanisms involved with a biological response to photofunctionalized Ti surfaces, in the current investigation, we addressed the question of whether or not UV-photofunctionalized Ti surfaces affected inflammatory markers expression by MC3T3-E1 cells. To the best of our knowledge, there is no evidence suggesting that inflammatory cytokines, such as the ones assessed in the present study, are modulated by UV-photofunctionalization. An inflammatory process occurs after implant placement, and macrophages play a crucial role in the wound healing process [43]. Macrophages can be dynamically induced to the pro-inflammatory M1 or anti-inflammatory M2 phenotype depending on the factors in the microenvironment [43–45]. In the early stage, IFN-γ can stimulate macrophages (M1) [45], which subsequently will secret proinflammatory cytokines such as TNF-α and IL-6 to keep with the inflammatory response to microbes and foreign bodies [43]. TNF-α and IL-6 expression may also be regulated by IL-17 [46], which regulates neutrophil homeostasis [47,48] and has also been reported to be involved in cell activation, growth, and proliferation [46], leading to an inflammatory process

or inflammation inhibition [44]. After 4-10 days, the anti-inflammatory mediators such as IL-4 can induce macrophages M2 [49,50], which promote vessel maturation, tissue repair [51] playing a critical role in wound healing response [44,52]. Therefore, the ability of a given material to modulate the inflammatory response may be a key factor controlling angiogenesis and tissue remodeling [53]. In general, the findings of the current investigation highlight the ability of certain surface treatment to regulate cytokines expression. Here, for the first time, UV photofunctionalized TiO_2 surfaces presented the potential to modulate inflammatory cytokine expression by pre-osteoblastic cells, suggesting that further studies should be considered in order to expand our knowledge on the potential of these surface treatment to promote biomineralization in unfavorable clinical conditions, including for example diabetes.

5. Conclusion

The current study addressed the hypothesis that UV-photofunctionalization affected physico-chemical and biological properties of Ti discs. Taken together, the findings of our study shed light on the potential of UV-photofunctionalized bi-phasic polycrystalline TiO_2 films to modify important physico-chemical characteristics of Ti-made discs' surface resulting in improved pre-osteoblastic cell differentiation and increased capacity to promote mineralization *in vitro*. In addition, UV-modified surfaces presented the ability to modulate the expression of key inflammatory markers.

Declarations of interest

None.

Acknowledgments

This study was financed in part by Coordenação de Aperfeiçoamento de Pessoal de Nível Superior - Brasil (CAPES) (Finance Code 001) and by the São Paulo State Research Foundation (FAPESP), Brazil (grant numbers 2016/06117-5). The authors express their gratitude to the Brazilian Nanotechnology National Laboratory (LNNano) at the Brazilian Center of Research in Energy and Materials (CNPEM) for the AFM facilities.

References

[1] H. Terheyden, N.P. Lang, S. Bierbaum, B. Stadlinger, Osseointegration - communication of cells, Clin. Oral Implants Res. 23 (2012) 1127–1135. https://doi.org/10.1111/j.1600-0501.2011.02327.x.

[2] K. Cheng, M. Yu, Y. Liu, F. Ge, J. Lin, W. Weng, H. Wang, Influence of integration of TiO2 nanorods into its nanodot films on pre-osteoblast cell responses, Colloids Surfaces B Biointerfaces. 126 (2015) 387–393. https://doi.org/10.1016/j.colsurfb.2014.12.002.

[3] M. Hatoko, S. Komasa, H. Zhang, T. Sekino, J. Okazaki, UV Treatment Improves the Biocompatibility and Antibacterial Properties of Crystallized Nanostructured Titanium Surface, Int. J. Mol. Sci. 20 (2019) 5991. https://doi.org/10.3390/ijms20235991.

[4] M. Kulkarni, A. Flasker, M. Lokar, K. Mrak-Poljšak, A. Mazare, A. Artenjak, S. Cucnik, S. Kralj, A. Velikonja, V. Kralj-Iglic, S. Sodin-Semrl, P. Schmuki, A. Iglič, Binding of plasma proteins to titanium dioxide nanotubes with different diameters, Int. J. Nanomedicine. 10 (2015) 1359. https://doi.org/10.2147/IJN.S77492.

[5] W. Att, N. Hori, F. Iwasa, M. Yamada, T. Ueno, T. Ogawa, The effect of UV-photofunctionalization on the time-related bioactivity of titanium and chromium-cobalt alloys, Biomaterials. 30 (2009) 4268–4276. https://doi.org/10.1016/j.biomaterials.2009.04.048.

[6] H. Aita, N. Hori, M. Takeuchi, T. Suzuki, M. Yamada, M. Anpo, T. Ogawa, The effect of ultraviolet functionalization of titanium on integration with bone, Biomaterials. 30 (2009) 1015–1025. https://doi.org/10.1016/j.biomaterials.2008.11.004.

[7] T. Kawano, W. Prananingrum, Y. Ishida, T. Goto, Y. Naito, M. Watanabe, Y. Tomotake, T. Ichikawa, Blue-violet laser modification of titania treated titanium: Antibacterial and osteo-inductive effects, PLoS One. 8 (2013) 1–7. https://doi.org/10.1371/journal.pone.0084327.

[8] N. Hori, F. Iwasa, N. Tsukimura, Y. Sugita, T. Ueno, N. Kojima, T. Ogawa, Effects of UV photofunctionalization on the nanotopography enhanced initial bioactivity of titanium, Acta Biomater. 7 (2011) 3679–3691. https://doi.org/10.1016/j.actbio.2011.06.022.

[9] H. Zhang, S. Komasa, C. Mashimo, T. Sekino, J. Okazaki, Effect of ultraviolet treatment on bacterial attachment and osteogenic activity to alkali-treated titanium with nanonetwork structures, Int. J. Nanomedicine. 12 (2017) 4633–4646. https://doi.org/10.2147/IJN.S136273.

[10] T. Miyauchi, M. Yamada, A. Yamamoto, F. Iwasa, T. Suzawa, R. Kamijo, K. Baba, T. Ogawa, The enhanced characteristics of osteoblast adhesion to photofunctionalized nanoscale TiO2 layers on biomaterials surfaces, Biomaterials. 31 (2010) 3827–3839. https://doi.org/10.1016/j.biomaterials.2010.01.133.

[11] Leon-Ramos, Diosdado-Cano, López-Santos, Barranco, Torres-Lagares, Serrera-Figallo, Influence of Titanium Oxide Pillar Array Nanometric Structures and Ultraviolet Irradiation on the Properties of the Surface of Dental Implants—A Pilot Study, Nanomaterials. 9 (2019) 1458. https://doi.org/10.3390/nano9101458.

[12] K.-H. Park, J.-Y. Koak, S.-K. Kim, S.-J. Heo, Wettability and cellular response of UV light irradiated anodized titanium surface, J. Adv. Prosthodont. 3 (2011) 63. https://doi.org/10.4047/jap.2011.3.2.63.

[13] K. Shahramian, A. Abdulmajeed, I. Kangasniemi, E. Söderling, T. Närhi, TiO 2 Coating

and UV Photofunctionalization Enhance Blood Coagulation on Zirconia Surfaces, Biomed Res. Int. 2019 (2019) 1–9. https://doi.org/10.1155/2019/8078230.

[14] J.-Y. Choi, C.J. Chung, K.-T. Oh, Y.-J. Choi, K.-H. Kim, Photocatalytic Antibacterial Effect of TiO 2 Film of TiAg on Streptococcus mutans, Angle Orthod. 79 (2009) 528–532. https://doi.org/10.2319/012108-169.1.

[15] H. Yaghoubi, N. Taghavinia, E.K. Alamdari, A.A. Volinsky, Nanomechanical Properties of TiO 2 Granular Thin Films, ACS Appl. Mater. Interfaces. 2 (2010) 2629–2636. https://doi.org/10.1021/am100455q.

[16] S. Cao, B. Liu, L. Fan, Z. Yue, B. Liu, B. Cao, Highly antibacterial activity of N-doped TiO2 thin films coated on stainless steel brackets under visible light irradiation, Appl. Surf. Sci. 309 (2014) 119–127. https://doi.org/10.1016/j.apsusc.2014.04.198.

[17] J.C. Lim, K.J. Song, C. Park, The effect of deposition parameters on the phase of TiO2 films grown by RF magnetron sputtering, J. Korean Phys. Soc. 65 (2014) 1896–1902. https://doi.org/10.3938/jkps.65.1896.

[18] V.A.R. Barão, M.T. Mathew, W.G. Assunção, J.C.-C. Yuan, M.A. Wimmer, C. Sukotjo, Stability of cp-Ti and Ti-6Al-4V alloy for dental implants as a function of saliva pH - an electrochemical study, Clin. Oral Implants Res. 23 (2012) 1055–1062. https://doi.org/10.1111/j.1600-0501.2011.02265.x.

[19] A.L.J. Pereira, P.N. Lisboa, J. Acuna, I.S. Brandt, A.A. Pasa, A.R. Zanatta, J. Vilcarromero, A. Beltran, J.H.D. da Silva, Enhancement of optical absorption by modulation of the oxygen flow of TiO2 films deposited by reactive sputtering, J. Appl. Phys. 111 (2012) 1–11. https://doi.org/10.1063/1.4724334.

[20] H.N. Pantaroto, A.P. Ricomini-Filho, M.M. Bertolini, J.H.D. Silva, N.F. Azevedo Neto, C. Sukotjo, E.C. Rangel, V.A.R. Barão, Antibacterial photocatalytic activity of different crystalline TiO2phases in oral multispecies biofilm, Dent. Mater. 34 (2018) e182–e195. https://doi.org/10.1016/j.dental.2018.03.011.

[21] I. Soriano, A.Y. Martín, C. Évora, E. Sánchez, Biodegradable implantable fluconazole delivery rods designed for the treatment of fungal osteomyelitis: Influence of gamma sterilization, J. Biomed. Mater. Res. Part A. 77A (2006) 632–638. https://doi.org/10.1002/jbm.a.30657.

[22] K. Subramani, R.T. Mathew, Titanium Surface Modification Techniques for Dental Implants—From Microscale to Nanoscale, in: Emerg. Nanotechnologies Dent., First Edit, Elsevier, 2012: pp. 85–102. https://doi.org/10.1016/B978-1-4557-7862-1.00006-7.

[23] M.H. Pham, M.A. Landin, H. Tiainen, J.E. Reseland, J.E. Ellingsen, H.J. Haugen, The effect of hydrofluoric acid treatment of titanium and titanium dioxide surface on primary human osteoblasts, Clin. Oral Implants Res. 25 (2014) 385–394. https://doi.org/10.1111/clr.12150.

[24] W.-E. Yang, H.-H. Huang, Multiform TiO2 nano-network enhances biological response to titanium surface for dental implant applications, Appl. Surf. Sci. 471 (2019) 1041–1052. https://doi.org/10.1016/j.apsusc.2018.11.244.

[25] M. Roy, A. Pompella, J. Kubacki, J. Szade, R.A. Roy, W. Hedzelek, Photofunctionalization of Titanium: An Alternative Explanation of Its Chemical-Physical Mechanism, PLoS One. 11 (2016) e0157481. https://doi.org/10.1371/journal.pone.0157481.

[26] E. Combe, A protocol for determining the surface free energy of dental materials, Dent. Mater. 20 (2004) 262–268. https://doi.org/10.1016/S0109-5641(03)00102-7.

[27] A.O. Matos, A.P. Ricomini-Filho, T. Beline, E.S. Ogawa, B.E.C. Oliveira, A.B. d. Almeida, F.H.N. Junior, E.C. Rangel, N.C. d. Cruz, C. Sukotjo, M.T. Mathew, V.A.R. Barão, Three-species biofilm model onto plasma-treated titanium implant surface, Colloids Surfaces B Biointerfaces. 152 (2017) 354–366. https://doi.org/10.1016/j.colsurfb.2017.01.035.

[28] I. da S.V. Marques, M.F. Alfaro, M.T. Saito, N.C. da Cruz, C. Takoudis, R. Landers, M.F. Mesquita, F.H. Nociti Junior, M.T. Mathew, C. Sukotjo, V.A.R. Barão, Biomimetic coatings enhance tribocorrosion behavior and cell responses of commercially pure titanium surfaces, Biointerphases. 11 (2016) 031008. https://doi.org/10.1116/1.4960654.

[29] T.L. Rodrigues, B.L. Foster, K.G. Silverio, L. Martins, M.Z. Casati, E.A. Sallum, M.J. Somerman, F.H. Nociti, Hypophosphatasia-associated Deficiencies in Mineralization and Gene Expression in Cultured Dental Pulp Cells Obtained from Human Teeth, J. Endod. 38 (2012) 907–912. https://doi.org/10.1016/j.joen.2012.02.008.

[30] G. Lecio, F.V. Ribeiro, S.P. Pimentel, A.A. Reis, R.V.C. da Silva, F. Nociti-Jr, L. Moura, E. Duek, M. Casati, R.C.V. Casarin, Novel 20% doxycycline-loaded PLGA nanospheres as adjunctive therapy in chronic periodontitis in type-2 diabetics: randomized clinical, immune and microbiological trial, Clin. Oral Investig. (2019). https://doi.org/10.1007/s00784-019-03005-9.

[31] I. Bertóti, M. Mohai, J.L. Sullivan, S.O. Saied, Surface characterisation of plasma-nitrided titanium: an XPS study, Appl. Surf. Sci. 84 (1995) 357–371. https://doi.org/10.1016/0169-4332(94)00545-1.

[32] V.K. Truong, S. Rundell, R. Lapovok, Y. Estrin, J.Y. Wang, C.C. Berndt, D.G. Barnes, C.J. Fluke, R.J. Crawford, E.P. Ivanova, Effect of ultrafine-grained titanium surfaces on adhesion of bacteria, Appl. Microbiol. Biotechnol. 83 (2009) 925–937. https://doi.org/10.1007/s00253-009-1944-5.

[33] K. Cai, M. Müller, J. Bossert, A. Rechtenbach, K.D. Jandt, Surface structure and composition of flat titanium thin films as a function of film thickness and evaporation rate, Appl. Surf. Sci. 250 (2005) 252–267. https://doi.org/10.1016/j.apsusc.2005.01.013.

[34] L.D. Trino, E.S. Bronze-Uhle, A. George, M.T. Mathew, P.N. Lisboa-Filho, Surface Physicochemical and Structural Analysis of Functionalized Titanium Dioxide Films, Colloids Surfaces A Physicochem. Eng. Asp. 546 (2018) 168–178. https://doi.org/10.1016/j.colsurfa.2018.03.019.

[35] R.A. Gittens, L. Scheideler, F. Rupp, S.L. Hyzy, J. Geis-Gerstorfer, Z. Schwartz, B.D. Boyan, A review on the wettability of dental implant surfaces II: Biological and clinical aspects, Acta Biomater. 10 (2014) 2907–2918. https://doi.org/10.1016/j.actbio.2014.03.032.

[36] D.A.H. Hanaor, C.C. Sorrell, Review of the anatase to rutile phase transformation, J. Mater. Sci. 46 (2011) 855–874. https://doi.org/10.1007/s10853-010-5113-0.

[37] D. CHODNIEWICZ, R. KLEMKE, Guiding cell migration through directed extension and stabilization of pseudopodia, Exp. Cell Res. 301 (2004) 31–37. https://doi.org/10.1016/j.yexcr.2004.08.006.

[38] T. Fujino, Y. Taguchi, S. Komasa, T. Sekino, M. Tanaka, Cell Differentiation on Nanoscale Features of a Titanium Surface: Effects of Deposition Time in NaOH Solution, J. Hard Tissue Biol. 23 (2014) 63–70. https://doi.org/10.2485/jhtb.23.63.

[39] M.F. López, J.A. Jiménez, A. Gutiérrez, XPS characterization of surface modified titanium alloys for use as biomaterials, Vacuum. 85 (2011) 1076–1079.

https://doi.org/10.1016/j.vacuum.2011.03.006.

[40] E.S. Bronze-Uhle, L.F.G. Dias, L.D. Trino, A.A. Matos, R.C. de Oliveira, P.N. Lisboa-Filho, Physicochemical characterization of albumin immobilized on different TiO2 surfaces for use in implant materials, Colloids Surfaces A Physicochem. Eng. Asp. 564 (2019) 39–50. https://doi.org/10.1016/j.colsurfa.2018.12.028.

[41] S.-H. Choi, W.-S. Jeong, J.-Y. Cha, J.-H. Lee, K.-J. Lee, H.-S. Yu, E.-H. Choi, K.-M. Kim, C.-J. Hwang, Effect of the ultraviolet light treatment and storage methods on the biological activity of a titanium implant surface, Dent. Mater. 33 (2017) 1426–1435. https://doi.org/10.1016/j.dental.2017.09.017.

[42] Y. Gao, Y. Liu, L. Zhou, Z. Guo, M. Rong, X. Liu, C. Lai, X. Ding, The Effects of Different Wavelength UV Photofunctionalization on Micro-Arc Oxidized Titanium, PLoS One. 8 (2013). https://doi.org/10.1371/journal.pone.0068086.

[43] L. Gao, M. Li, L. Yin, C. Zhao, J. Chen, J. Zhou, K. Duan, B. Feng, Dual-inflammatory cytokines on TiO 2 nanotube-coated surfaces used for regulating macrophage polarization in bone implants, J. Biomed. Mater. Res. Part A. 106 (2018) 1878–1886. https://doi.org/10.1002/jbm.a.36391.

[44] D.M. Mosser, J.P. Edwards, Exploring the full spectrum of macrophage activation, Nat. Rev. Immunol. 8 (2008) 958–969. https://doi.org/10.1038/nri2448.

[45] B.N. Brown, B.D. Ratner, S.B. Goodman, S. Amar, S.F. Badylak, Macrophage polarization: An opportunity for improved outcomes in biomaterials and regenerative medicine, Biomaterials. 33 (2012) 3792–3802. https://doi.org/10.1016/j.biomaterials.2012.02.034.

[46] D. V Jovanovic, J.A. Di Battista, J. Martel-Pelletier, F.C. Jolicoeur, Y. He, M. Zhang, F. Mineau, J.P. Pelletier, IL-17 stimulates the production and expression of proinflammatory cytokines, IL-beta and TNF-alpha, by human macrophages., J. Immunol. 160 (1998) 3513–21. http://www.ncbi.nlm.nih.gov/pubmed/9531313.

[47] M.A. Stark, Y. Huo, T.L. Burcin, M.A. Morris, T.S. Olson, K. Ley, Phagocytosis of Apoptotic Neutrophils Regulates Granulopoiesis via IL-23 and IL-17, Immunity. 22 (2005) 285–294. https://doi.org/10.1016/j.immuni.2005.01.011.

[48] J.J. Yu, M.J. Ruddy, G.C. Wong, C. Sfintescu, P.J. Baker, J.B. Smith, R.T. Evans, S.L. Gaffen, An essential role for IL-17 in preventing pathogen-initiated bone destruction: recruitment of neutrophils to inflamed bone requires IL-17 receptor–dependent signals, Blood. 109 (2007) 3794–3802. https://doi.org/10.1182/blood-2005-09-010116.

[49] A. Mantovani, S.K. Biswas, M.R. Galdiero, A. Sica, M. Locati, Macrophage plasticity and polarization in tissue repair and remodelling, J. Pathol. 229 (2013) 176–185. https://doi.org/10.1002/path.4133.

[50] K.L. Spiller, S. Nassiri, C.E. Witherel, R.R. Anfang, J. Ng, K.R. Nakazawa, T. Yu, G. Vunjak-Novakovic, Sequential delivery of immunomodulatory cytokines to facilitate the M1-to-M2 transition of macrophages and enhance vascularization of bone scaffolds, Biomaterials. 37 (2015) 194–207. https://doi.org/10.1016/j.biomaterials.2014.10.017.

[51] E. Conway, Molecular mechanisms of blood vessel growth, Cardiovasc. Res. 49 (2001) 507–521. https://doi.org/10.1016/S0008-6363(00)00281-9.

[52] S. Kumar, R. Meena, R. Paulraj, Role of Macrophage (M1 and M2) in Titanium-Dioxide Nanoparticle-Induced Oxidative Stress and Inflammatory Response in Rat, Appl. Biochem. Biotechnol. 180 (2016) 1257–1275. https://doi.org/10.1007/s12010-016-

2165-x.
[53] X. Yin, Y. Li, C. Yang, J. Weng, J. Wang, J. Zhou, B. Feng, Alginate/chitosan multilayer films coated on IL-4-loaded TiO2 nanotubes for modulation of macrophage phenotype, Int. J. Biol. Macromol. 133 (2019) 503–513. https://doi.org/10.1016/j.ijbiomac.2019.04.028.

3 DISCUSSÃO

O desenvolvimento de filmes protetores e bioativos para aplicação em implantes dentários tem se mostrado uma opção importante para garantir o sucesso do tratamento nos últimos anos. Nesta tese, filmes de TiO_2 em suas diferentes fases cristalinas foram depositados sobre a superfície do Ti por meio da pulverização catódica. Estes filmes foram capazes de aumentar a resistência à corrosão, bem como melhorar as propriedades biológicas do material.

Influência das diferentes fases cristalinas do TiO_2

Conforme esperado, as fases cristalinas do TiO_2 apresentaram diferentes influências nas propriedades da superfície, parâmetros eletroquímicos, adsorção de albumina e precipitação de hidroxiapatita. Em geral, as superfícies de TiO_2 composta por anatase e rutilo (mista) e a superfície composta unicamente por rutilo apresentaram o melhor comportamento para todos os testes eletroquímicos. A superfície de rutilo apresentou os menores valores de capacitância total (Q_{tot}), densidade de corrente de corrosão (i_{corr}) e taxa de corrosão, parâmetros relacionados à troca de íons entre o eletrólito e o substrato. Quanto menores forem esses valores, maior será a resistência à corrosão do material. Nesse caso, o filme funciona como uma barreira contra o transporte de espécies iônicas no eletrólito através da superfície, retardando o processo de degradação eletroquímica (Wang *et al.* 2015). Já se sabe que a fase rutilo é a mais estável, densa e resistente do TiO_2 cristalino (Diebold *et al.* 2003; Carp *et al.* 2004), o que pode ter garantido os resultados acima mencionados.

Já a fase mista deve ser destacada, pois apresentou resistência à polarização quase 6 ordens superior ao grupo controle, indicando uma extrema proteção contra a corrosão. Adicionalmente apresentou um ótimo comportamento de passivação, o que pode garantir estabilidade eletroquímica a longo prazo e menores taxas de degradação do material. Esse comportamento pode estar relacionado ao maior grau de cristalinidade (Kozlovskiy *et al.* 2019) obtido pela combinação das duas fases do TiO_2. Além disso, essa superfície pode ter um filme homogêneo com pequenos poros ou inexistentes e uma interface fortemente ligada

ao substrato (Ti), o que pode ser confirmado pelos maiores valores de η_{in} e pelo maior ângulo de fase em baixas frequências, resultando uma drástica inibição na propagação de corrosão por *pitting* (Shukla *et al.* 2017). As semelhantes propriedades entre as fases mista e rutilo podem ser explicadas pelas características da superfície.

Já a fase cristalina anatase exibiu a pior performance eletroquímica das superfícies de TiO_2, mas ainda assim, seus resultados foram superiores ao Ti não tratado. Algumas hipóteses podem explicar este comportamento. Primeiramente, o filme de anatase apresentou o potencial mais eletropositivo (OCP) entre as superfícies que apresentaram a maior diferença com o Ti não tratado. Essa diferença pode favorecer a ocorrência de corrosão galvânica entre o revestimento e o substrato (Wang *et al.* 2015). Em segundo lugar, a pequena quantidade de Ti e O observadas nas análises de XPS podem ser outro motivo, uma vez que o Ti tem uma afinidade muito alta com o O e a sua diminuição pode refletir em um baixo grau de cristalinidade (Kozlovskiy *et al.* 2019). Além disso, entre as superfícies de TiO_2, a anatase possui a menor dureza (Pantaroto *et al.* 2018) e é menos estável que os outros filmes, levando a um aumento em sua taxa de degradação.

Assim, é notável que a fase rutilo influencia positivamente na estabilidade eletroquímica dos filmes formados sobre o Ti. No entanto, a combinação das duas fases anatase e rutilo mostrou um comportamento protetor notável. Assim, controlar a quantidade de rutilo nos filmes mistos pode ser uma maneira de melhorar ainda mais a estabilidade eletroquímica dessa superfície, uma vez que aparentemente há uma maior quantidade de anatase no espectro da difração de raios-X da fase mista.

Com relação à morfologia encontrada nas superfícies estudadas, é possível notar a incorporação das nanopartículas de TiO_2, que são menores que 1 μm e costumam se organizar em aglomerados (Carp *et al.* 2004). O tamanho das nanopartículas variou de acordo com a fase cristalina (Hanaor *et al.* 2011). O rutilo apresentou partículas maiores em comparação às pequenas partículas de anatase, e na fase mista, é possível observar partículas de ambos os tamanhos, o que pode justificar sua maior rugosidade. A diferença no tamanho das partículas é devido ao processo de cristalinidade, no qual a partir do TiO_2 amorfo, primeiramente é formada a anatase, a qual pode então ser transformada e rutilo. O formato das partículas de rutilo sugere que suas partículas se formaram através da coalescência de várias partículas "anteriores" de anatase (Gouma *et al.* 2001), aumentando o tamanho dos grãos e reduzindo a área de superfície (Hanaor *et al.* 2011), justificando assim a mesma área de superfície encontrada em todas as superfícies do TiO_2.

Correlacionando a morfologia com a molhabilidade, já se sabe que a rugosidade da superfície pode influenciar diretamente em seu ângulo de contato. A maior rugosidade encontrada na fase mista refletiu em seu maior status hidrofílico. Adicionalmente, uma maior rugosidade e energia de superfície pode levar a uma maior interação com as proteínas (Gittens *et al.* 2014; Lorenzetti *et al.* 2015), o que também refletiu na fase mista, a qual apresentou a maior adsorção de albumina.

Uma maior cobertura de hidroxiapatita foi observada nas superfícies de TiO_2, o que já foi previamente descrito, uma vez que o TiO_2 apresenta maior bioatividade comparado à superfície do Ti puro (Liu *et al.* 2004; Lilja *et al.* 2011). Entretanto, as fases cristalinas do TiO_2 influenciaram na morfologia da hidroxiapatita, sendo as morfologias encontradas nas fases rutilo e mista mais interessantes para o processo de osseointegração (Lebre *et al.* 2017).

Considerando que a fase mista do TiO_2 composta de anatase e rutilo apresentou destaque quanto à resistência à corrosão, adsorção de albumina e bioatividade, esta foi a superfície escolhida para ser submetida ao tratamento de fotofuncionalização.

O TiO_2 misto associado à fotofuncionalização

A fotofuncionalização promoveu alterações significativas tanto na superfície do Ti, como na do TiO_2. Quanto à molhabilidade, houve uma redução no ângulo de contato de 53,5% no Ti e 74% no TiO_2, melhorando a molhabilidade das duas superfícies. Entretanto, a duração deste efeito foi curta, cerca de 1 hora após a aplicação da luz UV, ambas as superfícies já apresentaram valores no ângulo de contato próximos aos valores das respectivas superfícies não fotofuncionalizadas. Entretanto, isto pode ser evitado por até 28 dias, armazenando as superfícies fotofuncionalizadas em água destilada, assim as propriedades serão mantidas, evitando o envelhecimento da superfície (Choi *et al.* 2017).

Esta redução no ângulo de contato ocorre, pois a fotofuncionalização promove a redução no percentual atômico de carbono (Aita *et al.* 2009), que é um contaminante comumente presente na superfície do Ti e seus compostos (Bertóti *et al.* 1995). Após a fotofuncionalização, houve uma redução de carbono considerável na superfície do Ti e do TiO_2. Essa redução foi mais acentuada na superfície do TiO_2, possivelmente devido à sua propriedade fotocatalítica. O TiO_2 fotofuncionalizado apresentou apenas 8,5% de carbono em sua superfície, enquadrando-o como um metal de superfície "limpa" (Liu *et al.* 2004). A quantidade de carbono presente na superfície do implante no momento de sua implantação parece ser um dos fatores mais determinantes na afinidade inicial dos osteoblastos (Aita *et al.*

2009). Isto foi provado em nosso estudo, uma vez que as células apresentaram maior espalhamento, metabolismo e afinidade na superfície de TiO_2 fotofuncionalizada. Quanto à mineralização, ambas as superfícies Ti e TiO_2 fotofuncionalizadas apresentaram maiores taxas de mineralização comparado às superfícies não fotofuncionalizadas, o que pode ser decisivo nas propriedades biomecânicas do tecido ósseo a ser formado (Saruwatari *et al.* 2005). Sendo assim, o efeito da luz é benéfico para a mineralização celular, e o efeito da luz associado ao TiO_2 é benéfico para a adesão, espalhamento e viabilidade celular.

O melhor comportamento celular nas superfícies fotofuncionalizadas pode ser justificado pelo fato de que quando as superfícies são expostas à luz UV, ocorre a redução do carbono, e a consequente exposição dos sítios de Ti^{4+}, com isso, a superfície fica carregada positivamente, o que favorece a interação com as células osteoblásticas carregadas negativamente (Aita *et al.* 2009).

Tanto o TiO_2 como a fotofuncionalização não promoveram expressões exageradas em nenhuma das citocinas estudadas. Todas as superfícies expressaram IFN-γ, TNF-α, IL-4, IL-6 e IL-17, e esta expressão é considerada normal após a colocação de um implante, de forma a promover um processo inflamatório e consequentemente favorecer a cicatrização tecidual (de Oliveira *et al.* 2011). Considerando as poucas diferenças encontradas entre os grupos, é possível inferir que nem o TiO_2 nem a fotofuncionalização diferiram da expressão de citocinas do titânio, que é o material mais comumente utilizado na fabricação de implantes. Entretanto, é preciso considerar a complexidade do sistema imune e também lembrar que nem sempre o que ocorre *in vitro* acontecerá *in vivo.* Ainda há uma gama de citocinas para serem investigadas na presença do TiO_2 fotofuncionalizado, portanto, mais investigações são necessárias.

4 CONCLUSÃO

Os filmes de TiO_2 na fase cristalina mista (anatase e rutilo) são promissores para a aplicação nas superfícies dos implantes dentários, uma vez que melhoraram a resistência à corrosão do titânio, bem como aumentaram a adsorção de proteína, além de influenciarem positivamente na formação e morfologia da camada de hidroxiapatita. Além disso, o TiO_2 em sua fase mista foi capaz de potencializar o efeito da fotofuncionalização, o que refletiu em uma maior adesão, metabolismo e mineralização das células pré-osteoblásticas cultivadas nesta superfície, confirmando assim, a sua viabilidade. Quanto à expressão das citocinas

inflamatórias, foi constatado que tanto a fotofuncionalização, como o TiO_2 (associados ou não), não apresentaram consequências consideráveis na resposta inflamatória.

Extrapolando os nossos resultados para uma situação clínica, podemos inferir que a incorporação do TiO_2 cristalino misto na superfície dos implantes, seguido da fotofuncionalização, são tratamentos promissores, uma vez que aumentam a resistência do titânio, bem como podem acelerar o processo de osseointegração.

REFERÊNCIAS

Ahmed MH, Keyes TE, Byrne JA, Blackledge CW, Hamilton JW. Adsorption and photocatalytic degradation of human serum albumin on TiO2 and Ag–TiO2 films. J Photochem Photobiol A Chem. 2011 Jul;222(1):123–31. Available from: https://linkinghub.elsevier.com/retrieve/pii/S1010603011002255

Aita H, Hori N, Takeuchi M, Suzuki T, Yamada M, Anpo M, et al. The effect of ultraviolet functionalization of titanium on integration with bone. Biomaterials. 2009 Feb;30(6):1015–25. Available from: http://dx.doi.org/10.1016/j.biomaterials.2008.11.004

Att W, Hori N, Iwasa F, Yamada M, Ueno T, Ogawa T. The effect of UV-photofunctionalization on the time-related bioactivity of titanium and chromium-cobalt alloys. Biomaterials. 2009;30(26):4268–76. Available from: http://dx.doi.org/10.1016/j.biomaterials.2009.04.048

Bayón R, Igartua A, González JJ, Ruiz de Gopegui U. Influence of the carbon content on the corrosion and tribocorrosion performance of Ti-DLC coatings for biomedical alloys. Tribol Int. 2015 Aug;88:115–25. Available from: http://dx.doi.org/10.1016/j.triboint.2015.03.007

Beltrán-Partida E, Valdez-Salas B, Curiel-Álvarez M, Castillo-Uribe S, Escamilla A, Nedev N. Enhanced antifungal activity by disinfected titanium dioxide nanotubes via reduced

nano-adhesion bonds. Mater Sci Eng C. 2017 Jul;76:59–65. Available from: http://dx.doi.org/10.1016/j.msec.2017.02.153

Bertóti I, Mohai M, Sullivan JL, Saied SO. Surface characterisation of plasma-nitrided titanium: an XPS study. Appl Surf Sci. 1995 Apr;84(4):357–71. Available from: https://linkinghub.elsevier.com/retrieve/pii/0169433294005451

Bronze-Uhle ES, Dias LFG, Trino LD, Matos AA, de Oliveira RC, Lisboa-Filho PN. Physicochemical characterization of albumin immobilized on different TiO2 surfaces for use in implant materials. Colloids Surfaces A Physicochem Eng Asp. 2019 Mar;564(November 2018):39–50. Available from: https://doi.org/10.1016/j.colsurfa.2018.12.028

Cao S, Liu B, Fan L, Yue Z, Liu B, Cao B. Highly antibacterial activity of N-doped TiO2 thin films coated on stainless steel brackets under visible light irradiation. Appl Surf Sci. 2014 Aug;309:119–27. Available from: http://dx.doi.org/10.1016/j.apsusc.2014.04.198

Carp O, Huisman CL, Reller A. Photoinduced reactivity of titanium dioxide. Prog Solid State Chem. 2004;32(1–2):33–177.

Cheng K, Yu M, Liu Y, Ge F, Lin J, Weng W, et al. Influence of integration of TiO2 nanorods into its nanodot films on pre-osteoblast cell responses. Colloids Surfaces B Biointerfaces. 2015 Feb;126:387–93. Available from: https://linkinghub.elsevier.com/retrieve/pii/S092777651400678X

Choi J-Y, Chung CJ, Oh K-T, Choi Y-J, Kim K-H. Photocatalytic Antibacterial Effect of TiO 2 Film of TiAg on Streptococcus mutans. Angle Orthod. 2009 May;79(3):528–32. Available from: http://www.angle.org/doi/10.2319/012108-169.1

Choi S-H, Jeong W-S, Cha J-Y, Lee J-H, Lee K-J, Yu H-S, et al. Effect of the ultraviolet light treatment and storage methods on the biological activity of a titanium implant surface.

Dent Mater. 2017 Dec;33(12):1426–35. Available from: http://dx.doi.org/10.1016/j.dental.2017.09.017

Diebold U. The surface science of titanium dioxide. Surf Sci Rep. 2003;48(5):53–229.

Fojt J, Joska L, Málek J. Corrosion behaviour of porous Ti–39Nb alloy for biomedical applications. Corros Sci. 2013 Jun;71:78–83. Available from: https://linkinghub.elsevier.com/retrieve/pii/S0010938X13000863

Gabriel SB, Panaino JVP, Santos ID, Araujo LS, Mei PR, de Almeida LH, et al. Characterization of a new beta titanium alloy, Ti–12Mo–3Nb, for biomedical applications. J Alloys Compd. 2012 Sep;536(1):S208–10. Available from: http://dx.doi.org/10.1016/j.jallcom.2011.11.035

Gittens RA, Scheideler L, Rupp F, Hyzy SL, Geis-Gerstorfer J, Schwartz Z, et al. A review on the wettability of dental implant surfaces II: Biological and clinical aspects. Acta Biomater. 2014 Jul;10(7):2907–18. Available from: https://www.ncbi.nlm.nih.gov/pmc/articles/PMC3624763/pdf/nihms412728.pdf

Gouma PI, Mills MJ. Anatase-to-Rutile Transformation in Titania Powders. J Am Ceram Soc. 2001 Mar;84(3):619–22. Available from: http://doi.wiley.com/10.1111/j.1151-2916.2001.tb00709.x

Gowtham S, Arunnellaiappan T, Rameshbabu N. An investigation on pulsed DC plasma electrolytic oxidation of cp-Ti and its corrosion behaviour in simulated body fluid. Surf Coatings Technol. 2016 Sep;301:63–73. Available from: http://dx.doi.org/10.1016/j.surfcoat.2016.02.043

Hanaor DAH, Sorrell CC. Review of the anatase to rutile phase transformation. J Mater Sci. 2011;46(4):855–74.

Hatoko M, Komasa S, Zhang H, Sekino T, Okazaki J. UV Treatment Improves the Biocompatibility and Antibacterial Properties of Crystallized Nanostructured Titanium

Surface. Int J Mol Sci. 2019 Nov 28;20(23):5991. Available from: https://www.mdpi.com/1422-0067/20/23/5991

Hori N, Iwasa F, Tsukimura N, Sugita Y, Ueno T, Kojima N, et al. Effects of UV photofunctionalization on the nanotopography enhanced initial bioactivity of titanium. Acta Biomater. 2011;7(10):3679–91. Available from: http://dx.doi.org/10.1016/j.actbio.2011.06.022

Huang N, Yang P, Leng YX, Chen JY, Sun H, Wang J, et al. Hemocompatibility of titanium oxide films. Biomaterials. 2003 Jun;24(13):2177–87. Available from: https://linkinghub.elsevier.com/retrieve/pii/S0142961203000462

Kawano T, Prananingrum W, Ishida Y, Goto T, Naito Y, Watanabe M, et al. Blue-violet laser modification of titania treated titanium: Antibacterial and osteo-inductive effects. PLoS One. 2013;8(12):1–7.

Kokubo T, Takadama H. How useful is SBF in predicting in vivo bone bioactivity? Biomaterials. 2006 May;27(15):2907–15. Available from: https://linkinghub.elsevier.com/retrieve/pii/S0142961206000457

Kozlovskiy A, Shlimas I, Dukenbayev K, Zdorovets M. Structure and corrosion properties of thin TiO2 films obtained by magnetron sputtering. Vacuum. 2019 Jun;164:224–32. Available from: https://doi.org/10.1016/j.vacuum.2019.03.026

Kulkarni M, Flasker A, Lokar M, Mrak-Poljšak K, Mazare A, Artenjak A, et al. Binding of plasma proteins to titanium dioxide nanotubes with different diameters. Int J Nanomedicine. 2015 Feb;10:1359. Available from: http://www.dovepress.com/binding-of-plasma-proteins-to-titanium-dioxide-nanotubes-with-differen-peer-reviewed-article-IJN

Lebre F, Sridharan R, Sawkins MJ, Kelly DJ, O'Brien FJ, Lavelle EC. The shape and size of hydroxyapatite particles dictate inflammatory responses following implantation. Sci

Rep. 2017 Dec 7;7(1):2922. Available from: http://www.nature.com/articles/s41598-017-03086-0

Leon-Ramos, Diosdado-Cano, López-Santos, Barranco, Torres-Lagares, Serrera-Figallo. Influence of Titanium Oxide Pillar Array Nanometric Structures and Ultraviolet Irradiation on the Properties of the Surface of Dental Implants—A Pilot Study. Nanomaterials. 2019 Oct 14;9(10):1458. Available from: https://www.mdpi.com/2079-4991/9/10/1458

Li M, Gao L, Chen J, Zhang Y, Wang J, Lu X, et al. Controllable release of interleukin-4 in double-layer sol–gel coatings on TiO 2 nanotubes for modulating macrophage polarization. Biomed Mater. 2018 Apr 18;13(4):045008. Available from: http://stacks.iop.org/1748-605X/13/i=4/a=045008?key=crossref.8e37bf8f3aa7d474b8936ae57f375bc6

Lilja M, Genvad A, Åstrand M, Strømme M, Enqvist H. Influence of microstructure and chemical composition of sputter deposited TiO2 thin films on in vitro bioactivity. J Mater Sci Mater Med. 2011 Dec 4;22(12):2727–34. Available from: http://link.springer.com/10.1007/s10856-011-4465-6

Lim JC, Song KJ, Park C. The effect of deposition parameters on the phase of TiO2 films grown by RF magnetron sputtering. J Korean Phys Soc. 2014 Dec 7;65(11):1896–902. Available from: http://link.springer.com/10.3938/jkps.65.1896

Liu P, Hao Y, Zhao Y, Yuan Z, Ding Y, Cai K. Surface modification of titanium substrates for enhanced osteogenetic and antibacterial properties. Colloids Surfaces B Biointerfaces. 2017 Dec;160:110–6. Available from: https://doi.org/10.1016/j.colsurfb.2017.08.044

Liu X, Chu P, Ding C. Surface modification of titanium, titanium alloys, and related materials for biomedical applications. Mater Sci Eng R Reports. 2004 Dec 24;47(3–4):49–121. Available from: https://linkinghub.elsevier.com/retrieve/pii/S0927796X0400124X

López MF, Jiménez JA, Gutiérrez A. XPS characterization of surface modified titanium alloys for use as biomaterials. Vacuum. 2011 Jun;85(12):1076–9. Available from: http://dx.doi.org/10.1016/j.vacuum.2011.03.006

Lorenzetti M, Bernardini G, Luxbacher T, Santucci A, Kobe S, Novak S. Surface properties of nanocrystalline TiO 2 coatings in relation to the in vitro plasma protein adsorption. Biomed Mater. 2015 Jul 30;10(4):045012. Available from: http://stacks.iop.org/1748-605X/10/i=4/a=045012?key=crossref.45b90fd983d9e3c46fc3948b8252c64d

Marucco A, Fenoglio I, Turci F, Fubini B. Interaction of fibrinogen and albumin with titanium dioxide nanoparticles of different crystalline phases. J Phys Conf Ser. 2013 Apr 10;429(1):012014. Available from: http://stacks.iop.org/1742-6596/429/i=1/a=012014?key=crossref.cdb48a223f9202c93b5671e94a5ae310

Milleret V, Buzzi S, Gehrig P, Ziogas A, Grossmann J, Schilcher K, et al. Protein adsorption steers blood contact activation on engineered cobalt chromium alloy oxide layers. Acta Biomater. 2015 Sep;24:343–51. Available from: http://dx.doi.org/10.1016/j.actbio.2015.06.020

Miyauchi T, Yamada M, Yamamoto A, Iwasa F, Suzawa T, Kamijo R, et al. The enhanced characteristics of osteoblast adhesion to photofunctionalized nanoscale TiO2 layers on biomaterials surfaces. Biomaterials. 2010 May;31(14):3827–39. Available from: http://dx.doi.org/10.1016/j.biomaterials.2010.01.133

Mráz S, Schneider JM. Structure evolution of magnetron sputtered TiO2 thin films. J Appl Phys. 2011 Jan 15;109(2):023512. Available from: http://aip.scitation.org/doi/10.1063/1.3536635

Ochsenbein A, Chai F, Winter S, Traisnel M, Breme J, Hildebrand HF. Osteoblast responses to different oxide coatings produced by the sol–gel process on titanium substrates. Acta Biomater. 2008 Sep;4(5):1506–17. Available from: https://linkinghub.elsevier.com/retrieve/pii/S1742706108000883

Okazaki Y, Gotoh E. Comparison of metal release from various metallic biomaterials in vitro. Biomaterials. 2005 Jan;26(1):11–21. Available from: https://linkinghub.elsevier.com/retrieve/pii/S0142961204001267

Oliveira CMB, Sakata RK, Issy AM, Gerola LR, Salomão R. Cytokines and Pain. Brazilian J Anesthesiol. 2011 Mar;61(2):255–65. Available from: https://linkinghub.elsevier.com/retrieve/pii/S0034709411700290

Pantaroto HN, Ricomini-Filho AP, Bertolini MM, Silva JHD, Azevedo Neto NF, Sukotjo C, et al. Antibacterial photocatalytic activity of different crystalline TiO_2 phases in oral multispecies biofilm. Dent Mater. 2018;34(7):e182–95. Available from: https://doi.org/10.1016/j.dental.2018.03.011

Park K-H, Koak J-Y, Kim S-K, Heo S-J. Wettability and cellular response of UV light irradiated anodized titanium surface. J Adv Prosthodont. 2011;3(2):63. Available from: https://synapse.koreamed.org/DOIx.php?id=10.4047/jap.2011.3.2.63

Roy M, Pompella A, Kubacki J, Szade J, Roy RA, Hedzelek W. Photofunctionalization of Titanium: An Alternative Explanation of Its Chemical-Physical Mechanism. Mukherjee A, editor. PLoS One. 2016 Jun 16;11(6):e0157481. Available from: https://dx.plos.org/10.1371/journal.pone.0157481

Rupp F, Haupt M, Eichler M, Doering C, Klostermann H, Scheideler L, et al. Formation and Photocatalytic Decomposition of a Pellicle on Anatase Surfaces. J Dent Res. 2012;91(1):104–9. Available from: http://journals.sagepub.com/doi/10.1177/0022034511424901

Saruwatari L, Aita H, Butz F, Nakamura HK, Ouyang J, Yang Y, et al. Osteoblasts Generate Harder, Stiffer, and More Delamination-Resistant Mineralized Tissue on Titanium Than on Polystyrene, Associated With Distinct Tissue Micro- and Ultrastructure. J Bone Miner Res. 2005 Jul 11;20(11):2002–16. Available from: http://doi.wiley.com/10.1359/JBMR.050703

Shahramian K, Abdulmajeed A, Kangasniemi I, Söderling E, Närhi T. TiO 2 Coating and UV Photofunctionalization Enhance Blood Coagulation on Zirconia Surfaces. Biomed Res Int. 2019 Apr 1;2019:1–9. Available from: https://www.hindawi.com/journals/bmri/2019/8078230/

Shukla K, Rane R, Alphonsa J, Maity P, Mukherjee S. Structural, mechanical and corrosion resistance properties of Ti/TiN bilayers deposited by magnetron sputtering on AISI 316L. Surf Coatings Technol. 2017 Sep;324:167–74. Available from: http://dx.doi.org/10.1016/j.surfcoat.2017.05.075

Terheyden H, Lang NP, Bierbaum S, Stadlinger B. Osseointegration - communication of cells. Clin Oral Implants Res. 2012;23(10):1127–35.

Wang H, Zhang R, Yuan Z, Shu X, Liu E, Han Z. A comparative study of the corrosion performance of titanium (Ti), titanium nitride (TiN), titanium dioxide (TiO2) and nitrogen-doped titanium oxides (N–TiO2), as coatings for biomedical applications. Ceram Int. 2015 Nov;41(9):11844–51. Available from: https://linkinghub.elsevier.com/retrieve/pii/S0272884215010986

Westas E, Hayashi M, Cecchinato F, Wennerberg A, Andersson M, Jimbo R, et al. Bactericidal effect of photocatalytically-active nanostructured TiO 2 surfaces on biofilms of the early oral colonizer, Streptococcus oralis. J Biomed Mater Res Part A. 2017;105(8):2321–8. Available from: http://www.ncbi.nlm.nih.gov/pubmed/28380676

Yaghoubi H, Taghavinia N, Alamdari EK, Volinsky AA. Nanomechanical Properties of TiO 2 Granular Thin Films. ACS Appl Mater Interfaces. 2010 Sep 22;2(9):2629–36. Available from: https://pubs.acs.org/doi/10.1021/am100455q

Zhang H, Komasa S, Mashimo C, Sekino T, Okazaki J. Effect of ultraviolet treatment on bacterial attachment and osteogenic activity to alkali-treated titanium with nanonetwork structures. Int J Nanomedicine. 2017;12:4633–46.

ANEXOS

Anexo 1 – Verificação de originalidade e prevenção de plágio

Revestimento de TiO_2 cristalino na superfície do titânio: estabilidade eletroquímica e propriedades biológicas

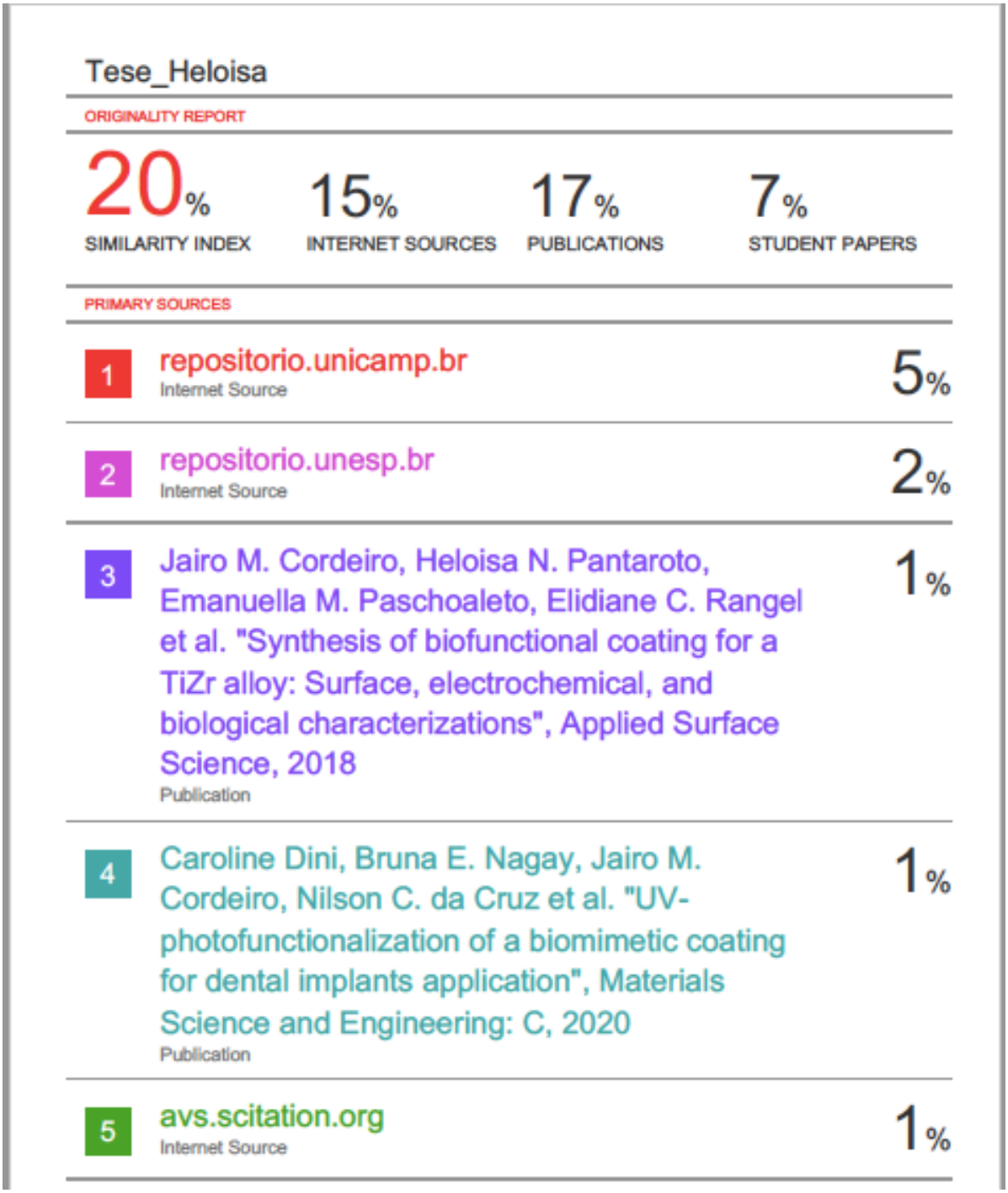

Tese_Heloisa

ORIGINALITY REPORT

20%	15%	17%	7%
SIMILARITY INDEX	INTERNET SOURCES	PUBLICATIONS	STUDENT PAPERS

PRIMARY SOURCES

1	repositorio.unicamp.br Internet Source	5%
2	repositorio.unesp.br Internet Source	2%
3	Jairo M. Cordeiro, Heloisa N. Pantaroto, Emanuella M. Paschoaleto, Elidiane C. Rangel et al. "Synthesis of biofunctional coating for a TiZr alloy: Surface, electrochemical, and biological characterizations", Applied Surface Science, 2018 Publication	1%
4	Caroline Dini, Bruna E. Nagay, Jairo M. Cordeiro, Nilson C. da Cruz et al. "UV-photofunctionalization of a biomimetic coating for dental implants application", Materials Science and Engineering: C, 2020 Publication	1%
5	avs.scitation.org Internet Source	1%

Anexo 2 – Comprovante de submissão do artigo

Confirm your agreement on your recent Co-Authored submission to APSUSC

Elsevier <eesserver@eesmail.elsevier.com>
Qua, 19/02/2020 07:49
Para: helopantaroto@hotmail.com <helopantaroto@hotmail.com>

Dear Dr. Heloisa N Pantaroto,

You have been listed as Co-Author of the following submission:

Journal: Applied Surface Science
Title: Outlining cell interaction and inflammatory cytokines on UV-photofunctionalized mixed-phase TiO2 thin film
Corresponding Author: Valentim A Barao
Co-Authors: Adaias O Matos; Amanda B de Almeida; Francisco H Nociti Jr.; Heloisa N Pantaroto; José Humberto D da Silva; Orisson P Gomes; Renato C Casarin; Richard Landers
Manuscript Number: APSUSC-D-20-02479

Elsevier asks co-authors to confirm their consent to be listed as co-author. In order to confirm your agreement to publish this article if it is accepted for publication, please click here:

https://ees.elsevier.com/copyright/Copyright.aspx?l=506556&s=HDDQIO2A

If you did not co-author this submission, please do not follow the above link but instead contact the Corresponding Author of this submission at vbarao@unicamp.br

Yours sincerely,

Applied Surface Science

****
For further assistance, please visit our customer support site at https://service.elsevier.com/app/home/supporthub/publishing/ Here you can search for solutions on a range of topics, find answers to frequently asked questions and learn more via interactive tutorials. You will also find our 24/7 support contact details should you need any further assistance from one of our customer support representatives.